CAVEOLAE AND CAVEOLIN-1 ARE IMPORTANT FOR VITAMIN D SIGNALLING

A Thesis
Presented to
The Academic Faculty

by

Kevin Wong

In Partial Fulfillment
of the Requirements for the Degree
Masters of Science in the
School of Biomedical Engineering

Georgia Institute of Technology
December 2010

CAVEOLAE AND CAVEOLIN-1 ARE IMPORTANT FOR VITAMIN D SIGNALLING

Approved by:

Dr. Barbara D. Boyan, Advisor
Wallace H. Coulter Department of Biomedical Engineering
Georgia Institute of Technology and Emory University

Dr. Hanjoong Jo
Wallace H. Coulter Department of Biomedical Engineering
Georgia Institute of Technology and Emory University

Dr. Zvi Schwartz
Wallace H. Coulter Department of Biomedical Engineering
Georgia Institute of Technology and Emory University

Dr. Janet E. Rubin
Department of Medicine
University of North Carolina Chapel Hill

Date Approved: August 24th, 2007

ACKNOWLEDGEMENTS

I wish to thank my advisors Dr. Boyan and Dr. Schwartz for their guidance. Also, without my parents; I would not be here today. Lastly, I would like to thank everyone who has shared their knowledge and their experiences in helping with my research.

TABLE OF CONTENTS

LIST OF TABLES

LIST OF FIGURES

LIST OF SYMBOLS AND ABBREVIATIONS

$1,25D_3$-MARRS	$1\alpha,25(OH)_2D_3$ Membrane Associated Rapid Response Steroid Binding
ERp60	Membrane $1\alpha,25(OH)_2D_3$ Receptor
RC	Resting/Reserve Zone Chondrocytes
GC	Growth Zone Chondrocytes
PKC	Protein Kinase C
VDR	nuclear receptor for $1\alpha,25(OH)_2D_3$
PLA_2	Phospholipase A_2
PLAP and PLAA	Phospholipase A_2 Activating Protein
PI-PLC	Phosphatidylinositol-Specific Phospholipase C
PLC	Phospholipase C
PIP_2	Phosphatidylinositol 4,5-bisphosphate
IP_3	Phosphoinositol Triphosphate
DAG	Diacylglycerol
Ca^{2+}	Calcium Ion
AA	Arachidonic Acid
MAPK	ERK1/2 Mitogen-Activated Protein Kinase
PLD	Phospholipase D
PGE_2	Prostaglandin E_2
MMPs	Matrix Metalloproteinases
Cav-1	Caveolin-1
Cav-2	Caveolin-2
Cav-3	Caveolin-3
DMEM	Dulbecco's Modified Eagle Medium

FBS	Fetal Bovine Serum
BSA	Bovine Serum Albumin
Cav-$1^{-/-}$	Cavoline-1 Knockout
Cav-$1^{+/+}$	Caveolin-1 Homozygous Wild type
$VDR^{-/-}$	VDR Knockout
$VDR^{+/+}$	VDR Homozygous Wild type
$VDR^{+/-}$	VDR Heterozygous
T.Ar	Total Tissue Area
B.Ar	Total Bone Area
B.Pm	Total Bone Perimeter
sL.Pm	Single-Labeled Perimeter
dL.Pm	Double-labeled Perimeter
Ir.L.Wi	Inter-Labeled Width
BV/TV	Trabecular Bone Volume
Tb.Th	Trabecular Thickness
Tb.N	Trabecular Number
sLS/BS	Single-Labeled Surface
dLS/BS	Double-Labeled Surface
MAR	Mineral Apposition Rate
BFR	Bone Formation Rate
TEM	Transmission Electron Microscopy
β-CD	Methyl-Beta-Cyclodextrin
TCA	Trichloroacetic Acid

SUMMARY

The most active form of Vitamin D, $1\alpha,25(OH)_2D_3$, modulates cells via receptor mediated mechanisms. While studies have elucidated the pathway via the classical nuclear Vitamin D Receptor (VDR), little is known about the membrane-associated Vitamin D Receptor (ERp60). Caveolae and its characteristic protein Caveolin-1 have been involved in many signaling pathways due to its specific structure and physical configuration. Other studies have shown that many components of the Vitamin D pathway have been found in caveolae. This study hypothesizes that caveolae and Caveolin-1 are important for the effects of 1,25 Vitamin D signaling via ERp60. Research up to date have shown that in rat and mouse growth zone chondrocytes, cells deprived of intact caveolae either through disruption through β-Cyclodextrin or genetic knockout do not exhibit the characteristic responses to Vitamin D through ERp60 when compared to chondrocytes with functional caveolae. Studies using immunofluorescence co-localization and caveolae fractionation have shown that ERp60 is localized in the caveolae domains. Cellular fractionation was also performed to examine the localization of the ERp60 receptor in lipid rafts and caveolae. Histology and transmission electron microscopy were also used to examine the physiological importance of caveolae and Caveolin-1 in growth plate morphology and cellular characteristics.

CHAPTER 1. INTRODUCTION

1.1 Background

Vitamin D metabolites have significant clinical importance in human physiology. The most commonly examined metabolites of vitamin D have been $1\alpha,25(OH)_2D_3$ and $24,25(OH)_2D_3$. Studies have shown a correlation between $1\alpha,25(OH)_2D_3$ and the immune system [1], cancer [2], bone formation [3], and mineral absorption [4]. Inhibition of vitamin D function through lack of sun exposure or genetic defects has led to the clinically manifested condition of rickets. Endochondral bone formation is particularly affected, and is characterized by bowing of the knees due to failure of the growth plate to become calcified.

Studies of vitamin D function have traditionally focused on the classical nuclear vitamin D receptor. While steroid hormones like vitamin D generally mediate transcription-associated events, they also participate in a more rapid, membrane-associated signaling phenomenon [3, 5, 6]. In the case of $1\alpha,25(OH)_2D_3$, $1,25D_3$-MARRS (Membrane associated, rapid response binding), also referred to as ERp60, has been identified as a membrane vitamin D receptor [7]. ERp60 is associated with many observed effects of $1\alpha,25(OH)_2D_3$ [8]. However, little is known about the location and the interaction of ERp60 within the plasma membrane where it initiates its membrane-associated effects.

1.2 Growth Plate

Cartilage, a relatively avascularized tissue, is produced by chondrocytes. Cartilage forms the necessary framework for many other tissues including bone, articular cartilage, and growth plate. The extracellular matrix produced by the cartilage consists

predominantly of type II collagen and proteoglycan, often in the form of proteoglycan aggregate with highly sulfated glycosaminoglycan side chains in mature tissues [9]. Chondrocytes will eventually undergo hypertrophy leading to mineralization of their extracellular matrix. The mineralized tissue is reabsorbed by osteoclasts, resulting in increased vascularization. Osteoprogenitor cells migrate to the mineralized tissue scaffold and form metaphyseal bone, characterized by bone trabeculae and bone marrow. Newly formed bone will eventually become reabsorbed leaving a marrow cavity. In some bones, between articular cartilage and the newly formed bone is the growth plate. In other bones, the growth plate is interposed between a secondary site of ossification and the metaphysic.

Bone growth occurs through one of two mechanisms: membranous ossification and endochondral ossification. In membranous ossification, bone growth occurs laterally in a direction perpendicular to the growth plate centers, and does not require the calcified cartilage for a scaffold. In endochondral bone formation, growth occurs longitudinally via the growth plate in a direction that results in the lengthening of bone. Growth plate morphology varies depending on its location in the body. There are also significant differences in the growth plate between animals of different species. In humans, the growth plate undergoes closure shortly after puberty. During the process, depending on the location of the growth plate, capillaries migrate through the calcified cartilage using osteoprogenitor cells that lay down trabecular bone; supporting marrow elements [4]. Although that same event occurs in rodents, the rodent growth plate remains permanently open.

The growth plate is characterized by a series of linearly aligned chondrocytes organized in clearly defined morphologic zones (Fig. 1). At one end of the growth plate is the resting-zone, or the reserve zone, where the chondrocytes exhibit a hyaline cartilage-like phenotype [9]. Cells in the resting-zone, also called RC cell, are scattered irregularly in the matrix. RC cells will remain in the resting-zone for an unknown amount of time until regulatory signals stimulate the cells to undergo proliferation. During the proliferative state, chondrocytes align, and they progress to a prehypertrophic state where significant changes occur to the shape and size of the cells. Additionally, chondrocytes also begin to modify their extracellular matrix [9]. In the hypertrophic cell zone, chondrocytes undergo a remarkable increase in size. The cytoplasm, endoplasmic reticulum, cisternae, golgi, and mitochondria also become greatly enlarged [10]. While the extracellular matrix produced by chondrocytes in the proliferation and the prehypertrophic zones have low levels of mineral content, there is increasingly more mineral content in the last three to four cell layers in the lower hypertrophic zone [11]. Hypertrophic cells also exhibit signs of apoptosis [4]. Pre-hypertrophic and hypertrophic zones are collectively referred to as growth zones, and the cells contained in them are referred to as growth zone chondrocytes, or GC cells. Beyond the hypertrophic zone, the matrix vesicles in the extracellular matrix begin to form apatite crystals leading to calcified cartilage that will eventually pave the way for bone deposition.

1.3 Regulation by Vitamin D_3

Pre-vitamin D_3 is produced from 7-dehydrocholesterol, a derivative of cholesterol, via a photochemical process in the skin. Vitamin D_3 is then formed via the spontaneous isomerization of pre-vitamin D_3. Another source of vitamin D_3 is via

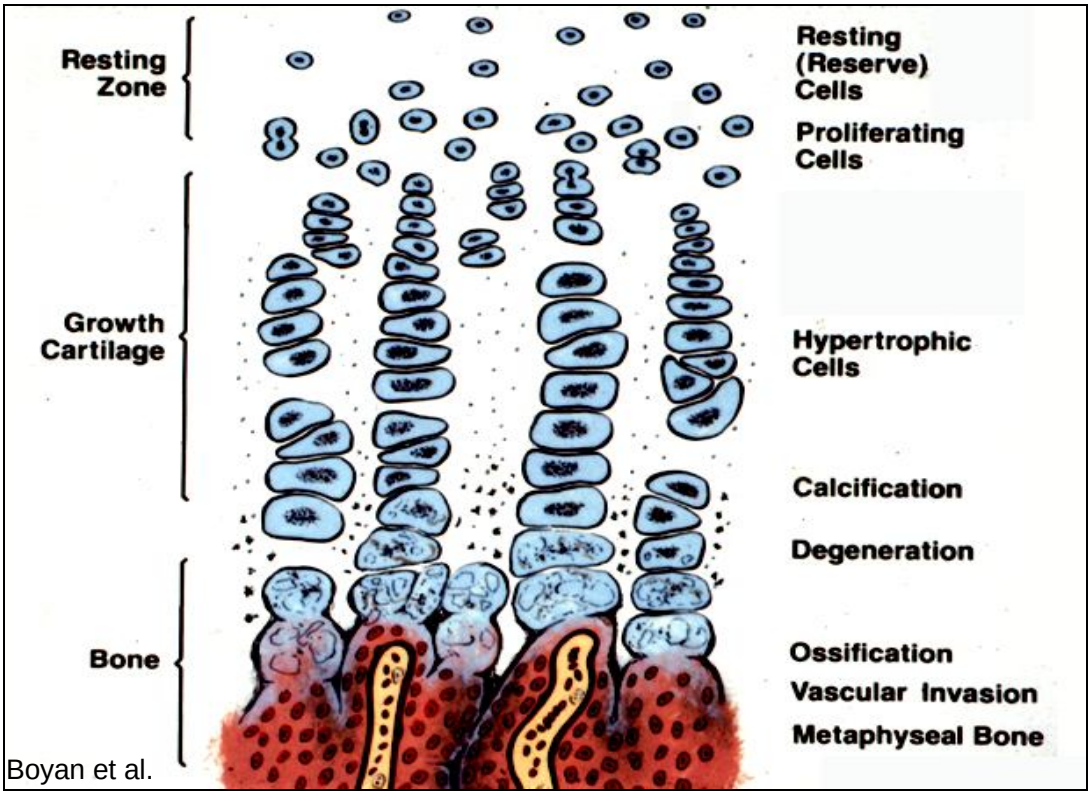

Figure 1. Schematic of the growth plate

fortified foods such as milk and cereal. Regardless of the source of vitamin D_3, it is hydroxylated in the liver to 25-hydroxyvitamin D_3 [$25(OH)D_3$]. Further hydroxylation in the kidney results in the production of the two main biologically active forms of vitamin D: $1\alpha,25(OH)_2D_3$ and $24R,25(OH)_2D_3$. Vitamin D_3 has a significant and important association with cartilage. In studies where vitamin D deficient rats are treated with radiolabeled $25(OH)_2D_3$, $1\alpha,25(OH)_2D_3$ and $24,25(OH)_2D_3$ accumulated within the tissue [9]. Additionally, it was found that even though the circulating levels of these vitamin D metabolites are at the picomolar levels, their levels in the growth plate are in the nanomolar range [12].

$1\alpha,25(OH)_2D_3$ has a very important role in mineral metabolism. It is involved in the intestinal absorption of calcium and phosphorus, enhancement of renal mineral absorption, stimulation of osteoclastic bone resportion, and promotion of mineral deposition in newly mineralized bone [4]. Within the growth plate, $1\alpha,25(OH)_2D_3$ has two major functions; it modulates calcium transport to the extracellular matrix and crystal formation in matrix vesicles [13], and it promotes the differentiation of prehypertrophic and hypertrophic chondrocytes. The biological role of $24,25(OH)_2D_3$ is not as well understood, and there have been controversies over its significance [14]. However, studies have shown that both of the vitamin D metabolites activate the protein kinase C (PKC) signaling pathway in their respective target cells [15, 16]. The classical nuclear receptor for $1\alpha,25(OH)_2D_3$ (VDR) has been found in growth plate chondrocytes, though the nuclear receptor for $24,25(OH)_2D_3$ has not been elucidated. Studies have shown that receptors for both $1\alpha,25(OH)_2D_3$ and $24,25(OH)_2D_3$ have been found in the plasma membrane and the matrix vesicles of growth plate chondrocytes [17, 18]. The vitamin D

metabolites, however, affect cells differently and through different signaling mechanisms. While the activation of the PKC signaling cascade via $1\alpha,25(OH)_2D_3$ has been found in prehypertropic and hypertrophic cells, $24,25(OH)_2D_3$ activation of PKC has been found in RC cells.

Clinically, vitamin D has been very effective in treating rickets. In rickets, the vitamin D deficiency results in the failure of hypertrophic cartilage calcify its matrix. Rickets does not cause significant changes in the proliferating cell zone. Instead, prehypertrophic chondrocytes fail to mature, resulting in elongation of the hypertrophic zone. Even though mineralization still occurs despite vitamin D deficiency, studies have shown the mineral crystals that are formed in rachitic mice are less mature than those of normal rats [19]. The inability of the cartilage to become calcified is primarily due to the failure of the cells to transport calcium effectively.

Raising the Ca^{2+} ion content of the serum has been shown to heal mineralization defects [20]. However, vitamin D is also involved in the regulation of other aspects of growth plate physiology that may contribute to the development of rickets. The lipid metabolism of the growth plate is altered in vitamin D deficiency, and treatment of rachitic chicks with vitamin D causes an increase in the activity of phospholipase A_2 in the growth plate [9]. Additionally, changes in the regulation of matrix vesicle enzymes such as alkaline phosphatase and matrix metalloproteinases may also play a role in rickets. Alkaline phosphatase activity normally increases through the hypertrophic zone, but rachitic animals have a suppressed level of activity that can be rapidly increased with $1\alpha,25(OH)_2D_3$ [9]. Proteoglycans, a major component of the extracellular matrix, form smaller aggregates in vitamin D deficit chicks [21]. Vitamin D deficiency has also been

linked to altered rate of cartilage resorption and altered regulation of osteoclast formation [9].

It is still unclear how different metabolites of vitamin D regulate the growth plate. While $1\alpha,25(OH)_2D_3$ will heal rachitic lesions by affecting calcium regulation, $24,25(OH)_2D_3$ has also been found to heal rickets through a different mechanism. It is likely that $24,25(OH)_2D_3$ acts directly on the chondrocytes in the upper growth plate to promote differentiation along the endochondral lineage. The healing effect of $1\alpha,25(OH)_2D_3$ increases with the addition of $24,25(OH)_2D_3$ [22].

1.4 Rapid Actions and Nongenomic Mechanisms of Vitamin D_3

Both $1\alpha,25(OH)_2D_3$ and $24,25(OH)_2D_3$ exert many of their effects on cartilage via VDRs that involve changes in gene transcription and mRNA stabilization [9]. However, there is also evidence of membrane-mediated mechanisms with nongenomic actions. In nongenomic actions, the hormone is not involved in the regulation of new gene transcription or protein synthesis. Due to the ability for rapid protein synthesis, it is not sufficient to consider nongenomic actions as rapid actions. Instead, experiments examine membrane fluidity, rapid turnover of phospholipids, changes in calcium flux, and rapid activation of PKC as proof of nongenomic actions. The difference in charge density between $1\alpha,25(OH)_2D_3$ and $24,25(OH)_2D_3$ results in different interactions with the membrane, resulting in different fluid mosaic structures. Treatment of RC and GC cells with $1\alpha,25(OH)_2D_3$ and $24,25(OH)_2D_3$ causes changes in membrane fluidity in a cell specific manner [23]. $1\alpha,25(OH)_2D_3$ increases the fluidity of GC plasma membranes, but does not change the membrane fluidity of RC cell. On the other hand, $24,25(OH)_2D_3$ decreases the membrane fluidity of GC cells while increasing the fluidity of RC plasma

membranes. The most compelling evidence for the membrane action of 1α,25$(OH)_2D_3$ and 24,25$(OH)_2D_3$ is the capability of growth plate cartilage cells from vitamin D receptor knockout mice to preserve their membrane response to 1α,25$(OH)_2D_3$ and 24,25$(OH)_2D_3$ [5].

1.5 Mechanism of Action

1.5.1 1,α25$(OH)_2D_3$

The rapid action of 1α,25$(OH)_2D_3$ on GC cells is shown in Fig. 2 [9] and is summarized below. The mechanism involves ERp60, causing a rapid increase in phospholipase A_2 (PLA_2) activity. The increase in PLA_2 is dependent on the activity of PLA_2 activating protein, also named PLAP and PLAA. PLAA results in increased fatty acid turnover, which in turn leads to increased membrane fluidity [9]. Additionally, the fluidity change alters membrane enzyme activity and calcium ion flux [24]. The lysophospholipids released by PLAA activate phosphatidylinositol-specific phospholipase C (PI-PLC). PLC then catalyzes the hydrolysis of phasphotidylinositol 4,5-bisphosphate (PIP_2), increasing production of phosphoinositol trisphosphate (IP_3), and leaving diacylglycerol (DAG) associated with the membrane [25]. IP_3 is involved in calcium regulation by causing the release of Ca^{2+} from the endoplasmic reticulum into the cytoplasm. DAG will bind to PKC, causing its translocation to the plasma membrane. DAG, together with Ca^{2+}, will also activate PKC. PLA_2 also leads to the stimulation of arachidonic acid (AA) release. AA release can stimulate PKC activity; it is the rate-limiting step in prostaglandin production in response to 1α,25$(OH)_2D_3$, and its release results in increased prostaglandin E_2 (PGE_2) production, which is an autocrine

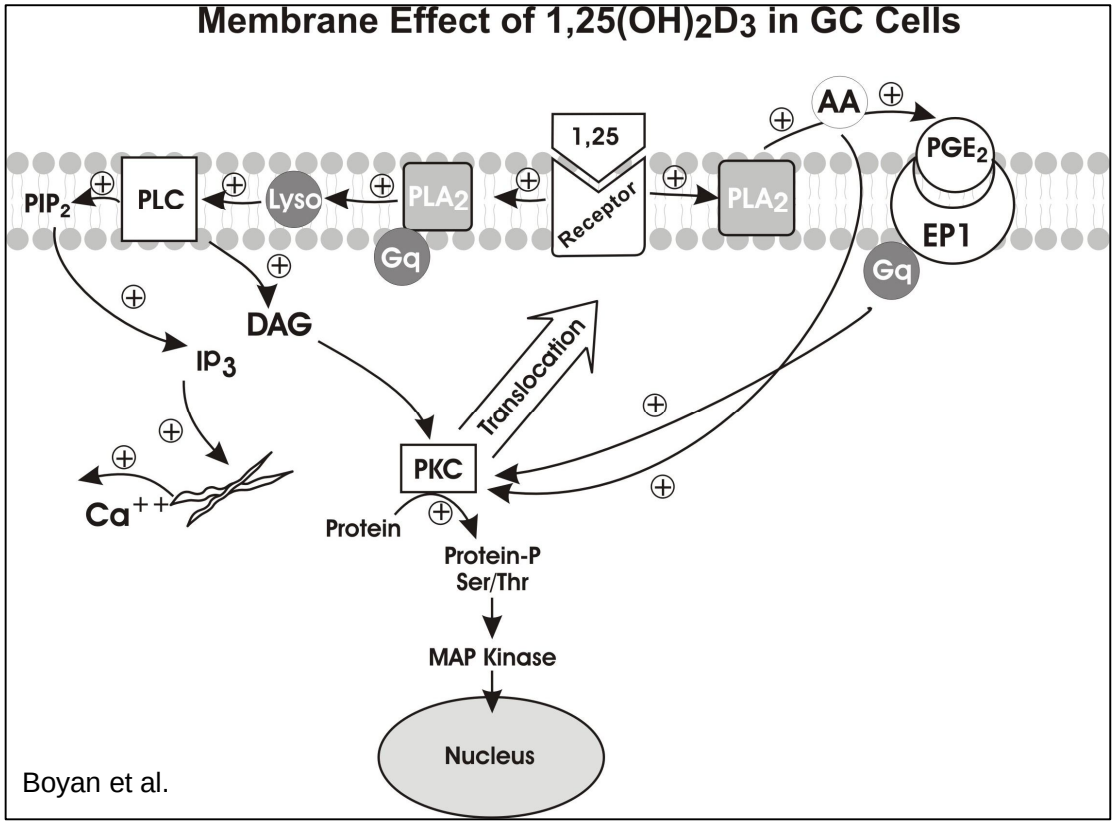

Figure 2. Membrane action of 1α,25$(OH)_2D_3$ in GC cells

factor that acts on PKC via its EP1 receptor [9]. PKC activation initiates phosphorylation of signaling cascades that lead to the activation of ERK1/2 mitogen-activated protein kinase (MAPK), and the phosphorylation of AP-1 sites on the related gene promoters [26].

1.5.2 24,25(OH)$_2$D$_3$

The rapid action of 24R,25(OH)$_2$D$_3$ on RC cells is shown in Fig. 3 [27] and is summarized below. While the membrane receptor for 1α,25(OH)$_2$D$_3$ has been identified as ERp60, the identity of the membrane receptor for 24,25(OH)$_2$D$_3$ is not known. However, studies have shown that 24,25(OH)$_2$D$_3$ signaling in RC cells, contrary to 1α,25(OH)$_2$D$_3$ binding to GC cells, inhibits PLA$_2$ activity [24]. The altered PLA$_2$ affects the cells through mechanisms already described above. The effects include changes in membrane fluidity, changes in fatty acid turnover, release of arachidonic acid, a change in Ca^{2+} flux, an increase in DAG production, and production of PGE$_2$ [9]. DAG can subsequently activate PKC, but the activation does not result in the translocation of PKC to the plasma membrane. 24,25(OH)$_2$D$_3$ does not lead to changes in PLC activity, and inhibiting PLC activity does not result in altered PKC response to 24,25(OH)$_2$D$_3$ [28]. Contrary to 1α,25(OH)$_2$D$_3$ signaling in GC cells, inhibition of PLA$_2$ leads to increased PKC activity, and the introduction of exogenous AA, lysophospholipid, PLA$_2$, and PGE$_2$ all inhibit PKC [9]. The effect of PGE$_2$ via EP2 is through protein kinase A (PKA). While PLC does not play a substantial role in PKC activation in RC cells, phospholipase D (PLD) has a much more prominent role. Activation of PLD results in the increased production of DAG and activation of PKC, which leads to phosphorylation of MAPK and translocation of MAPK to the nucleus for activation of transcription [27].

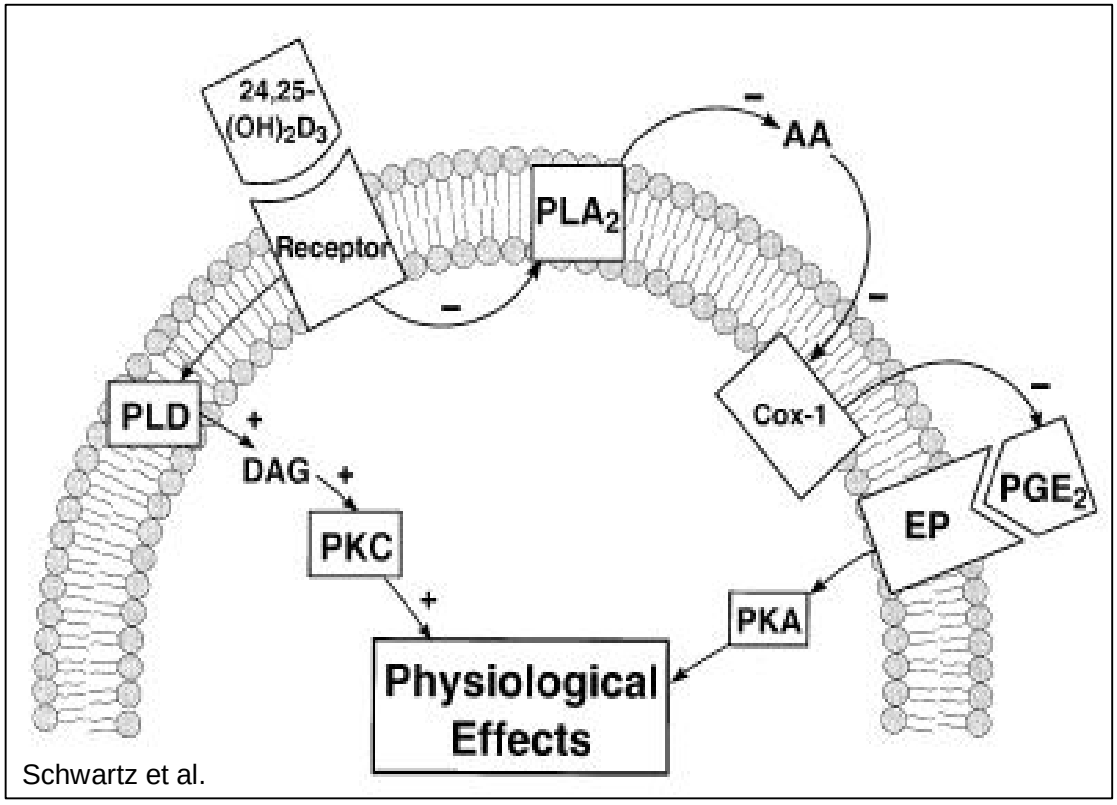

Figure 3. Membrane action of $24,25(OH)_2D_3$ in RC cells

1.6 Regulation of Matrix Vesicles

The matrix composition varies greatly between the resting zone and the growth zone. At the upper hypertrophic zone, the chondrocytes begin to modify their extracellular matrix to facilitate the eventual increase in the size of the cells. The sulfated proteoglycan aggregates are degraded by matrix metalloproteinases (MMPs) and new matrix is produced that contains type X collagen [29]. Calcification occurs at the bottom of the hypertrophic zone. Regulation of the matrix, in addition to the matrix content, varies between cells in the resting zone and cells in the growth zone. They are able to regulate events that occur in the matrix through activation of enzymes such as the aforementioned MMPs. Additional differences between RC and GC cell regulation of the extracellular matrix include lowered lipid composition in the matrix vesicle membrane of cultured RC cells when compared to cultured GC cells [23].

1α,25$(OH)_2D_3$ and 24,25$(OH)_2D_3$ regulate the extracellular matrix of chondrocytes via genomic pathways. 1α,25$(OH)_2D_3$ and 24,25$(OH)_2D_3$ regulate matrix synthesis and matrix vesicle composition in GC and RC cells, respectively [30]. The matrix vesicles have become excellent models for studying nongenomic actions of vitamin D due to their position exterior to the cell and the lack of DNA or RNA. Using the matrix vesicle model, we have shown that 1α,25$(OH)_2D_3$ and 24,25$(OH)_2D_3$ regulate PLA_2 activity in a cell-specific manner [30]. While 1α,25$(OH)_2D_3$ stimulates PLA_2 activity in matrix vesicles isolated from cultured GC cells, 24,25$(OH)_2D_3$ inhibits PLA_2 specific activity in matrix vesicles isolated from cultured RC cells. The nongenomic regulation of the extracellular matrix by vitamin D is hypothesized in Fig 4 and summarized below [9]. In addition to regulated matrix production via genomic and

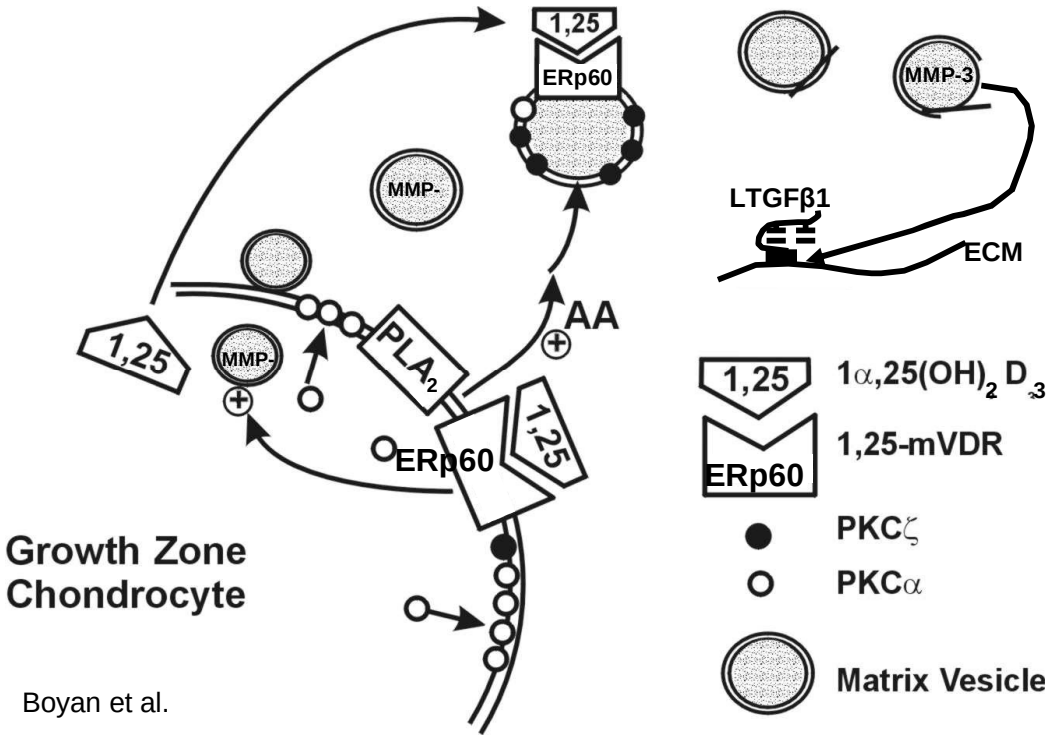

Figure 4. Regulation of matrix vesicles by $1\alpha,25(OH)_2D_3$

nongenomic pathways, vitamin D metabolites are synthesized by cells and secreted in response to regulatory factors like $1\alpha,25(OH)_2D_3$, $24,25(OH)_2D_3$, or TGF-β_1. The vitamin D metabolites diffuse freely into the matrix and interact with the plasma membrane and the matrix vesicle membrane. In the matrix vesicles, this interaction initiates biochemical pathways that lead to the maturation of matrix vesicles, hydroxyapatite crystal formation, degeneration of the integrity of the matrix vesicle membranes, and release of active proteases such as metalloproteinases (MMP). The proteases are capable of degrading matrix proteoglycans and facilitating matrix calcification. Lastly, they can also act on latent growth factors such as latent TGF-β_1 (LTGF-β_1) to act in autocrine or paracrine manners.

1.7 Caveolae and Vitamin D

Caveolae are unique membrane domains that are characterized by a cave-like invagination as seen via electron miscroscopy and by proteins caveolin-1, 2, and 3. The exact role and function of caveolae and its characteristic proteins are unclear, but they have been implicated in many biological functions. At least part of caveolae's functions is derived from its unique membrane composition. While the lipid bilayer of the plasma membrane has been viewed as a two-dimensional "fluid mosaic" model with loosely pack phospholipid bilayer capable of rapid lateral diffusion, caveolae exist in "liquid-ordered" states where the bilayer assembly is more rigid and with confined movement of the lipid bilayer. This characteristic is attributed to a confluence of cholesterol and sphingolipids in the caveolae domains. Caveolae have been classified as a sub-domain of lipid rafts in the past due to similar lipid and cholesterol components. However, studies have begun to separate the functions of caveolae from lipid rafts starting with the exclusivity of caveolin

proteins in caveolae [31]. The unique lipid compositions of caveolae and lipid rafts have allowed the isolation of these membrane domains through their resistance to solubilization by mild nonionic detergents such as Triton X-100 [32]. However, studies have shown that the detergents can extract certain molecules from caveolae/lipid raft domains, and a sucrose-based gradient extraction method that takes advantage of the lower density found in the caveolae/lipid raft fractions is more commonly used to obtain fractions that are more pure [33].

Caveolae and caveolin-1, 2, and 3 are located in many tissues and are implicated in many cellular and physiological functions. However, the presence and the role of caveolae and caveolin-1, 2, and 3 are not ubiquitous and vary between different biological components. While caveolae are found in most tissues including human knee joint cartilage [34], they are noticeably absent in central nervous system neurons [35]. The presence of caveolin-1, 2, and 3 also varies significantly with caveolin-3 found mostly in musculoskeletal cells and caveolin-2 found exclusively in conjunction with caveolin-1 (Cav-1) [36]. Current knowledge has implicated caveolae/caveolins in many biological functions [37]: vesicular transport such as transcytosis, endocytosis, and protocytosis; cellular cholesterol homeostasis such as transport of synthesized cholesterol and cholesterol efflux from cells; oncogenes and tumorigenesis such as caveolins as tumor suppressors and as targets of oncogenes; and signaling transduction mechanisms such as caveolin as modulators of signaling and compartmentalized signaling.

Caveolae have already been found to contain nuclear VDR, implicating an important role for the plasma membrane in vitamin D signaling [38]. Additionally, Cav-1 has been identified to play an important role in the function of membrane-associated

estrogen receptors [39, 40]. Many of the components of the ERp60-dependent PKC signaling pathway have been found in lipid rafts and caveolae, including PLA_2 [41], PLC [42], DAG, annexin II [43], and PKC [44]. Studies have also linked PLAA, an important and early activator/inhibitor of vitamin D signaling, to G proteins [45]. This is particularly interesting and can serve as an insight into the role of caveolae in vitamin D signaling due to interactions of many G proteins with caveolae [37].

CHAPTER 2. MATERIALS AND METHODS

2.1 Cell Culture

Resting zone and growth zone chondrocytes were isolated from their respective zones in the costochondral cartilages of 125-g male Sprague-Dawley rats [24]. Chondrocytes were cultured in Dulbecco's modified Eagle medium (DMEM) containing 10% fetal bovine serum (FBS), 1% antibiotics, and 50 μg/ml ascorbic acid. Resting zone cells were plated at 10,000 cells/cm^2 and growth zone cells were plated at 25,000 cells/cm^2. Confluent cultures (approximately 7 days after seeding) were sub-passaged at the same seeding densities. Media were changed at 24 hours and then at 72 hour intervals. Confluent fourth passage cells were used for all experiments. Numerous published papers show that these cells retain their chondrocyte phenotype at this passage. In addition, fourth passage cells continue to display differential responsiveness to $1\alpha,25(OH)_2D_3$ as well as to other regulatory agents [3, 24, 26].

To culture growth plate chondrocytes from the wild type and Cav-$1^{-/-}$ mice, we adapted techniques originally established for $VDR^{-/-}$ mice [5]. Rib cages were removed from eight-week old wild type and Cav-$1^{-/-}$ mice. Resting zone and growth zone cartilage were separated by sharp dissection under a microscope. Cells were seeded at the same densities used for the rat chondrocytes and were cultured in DMEM containing FBS, antibiotics and vitamin C, but the amount of FBS was increased to 15%.

2.2 Animal Models

To determine the requirement for lipid rafts/caveolae in the response to $1\alpha,25(OH)_2D_3$, we used cartilage cells isolated from costochondral cartilages from 125-g male Sprague Dawley rats [23]. Rats of this size are young adults but the growth plate

cartilages remain open. Male 8-week-old Cav-$1^{-/-}$ mice [36, 46] were used to address the role of caveolin-1 in the mechanism. These mice were maintained in the transgenic mouse facility at Emory University Medical School (Atlanta, GA). Cav-$1^{-/-}$ mice lack caveolae based on transmission electron microscopy (TEM) of the plasma membranes of their endothelial cells. They exhibit impaired nitric oxide and calcium signaling in the cardiovascular system. In addition, their lungs display thickening of alveolar septa caused by uncontrolled endothelial cell proliferation and fibrosis [36, 47]. The musculoskeletal phenotype in the Cav-$1^{-/-}$ mice has not been described. Male 8-week-old wild-type C57BL/6 mice (Jackson Labs, Bar Harbor, Maine) were used as controls. A mouse colony was established in the Laboratory Animal Research Center at Georgia Institute of Technology using a heterozygous ($VDR^{+/-}$) breeding pair obtained as a gift from Dr. Marie Demay (Harvard Medical School, Massachusetts General Hospital, Boston, MA). The phenotypic characteristics of these mice have been described in detail in a series of publications [48-50]. Offspring were genotyped at two weeks after birth. $VDR^{+/-}$ mice were allowed to breed. Homozygous wildtype ($VDR^{+/+}$) and 1,25-nVDR knockout ($VDR^{-/-}$) mice were euthanized when 8 weeks old. $VDR^{-/-}$ mice exhibited phenotypic markers of vitamin D deficiency, including rachitic growth plates with expanded hypertrophic cell zones.

2.3 Morphometric Study

Five Cav-$1^{+/+}$ and four Cav-$1^{-/-}$ mice at 8 weeks of age were used for morphometric study. Calcein (25 mg/kg body weight; Sigma Chemical Co., St. Louis, MO) was injected intraperitoneally at 6 and 2 days before harvest. After euthanasia, the right leg was dissected and the femur was separated from the skin and the muscle. The

femur was then fixed in 70% ethanol and stored in the dark at 4°C. Following dehydration in a graded series of ethanol (70%, 95%, and 100%), the femur was infiltrated and embedded without decalcification in methylmethacrylate. A longitudinal mid-section of the femur was cut at a thickness of 5 μm with a 355HM Microtome (Micom, UK). The area measured was defined by the cortical bone on both sides and by growth plates at each end of the bone. Histomorphometric analysis was performed with Leica DMLB microscope and images taken with Leica DC300 camera (Chatsworth, California). The following parameters were measured using NIH Image pro Plus software. In the trabecular bone, total tissue area (T.Ar, μm^2), total trabecular bone area (B.Ar, μm^2), total trabecular bone perimeter (B.Pm, μm), single-labeled bone perimeter (sL.Pm, μm), double-labeled bone perimeter (dL.Pm, μm), and interlabeled width (Ir.L.Wi, μm). The following parameters were calculated: trabecular bone volume (BV/TV, %), trabecular thickness (Tb.Th, μm), trabecular number (Tb.N, number/μm), single-labeled surface (sLS/BS, %), double-labeled surface (dLS/BS, %), mineral apposition rate (MAR, μm/day), and bone formation rate (BFR/BS, 1022 $\mu m^3/\mu m^2$/day). In the cortical bone, total cortical bone area (B.Ar, μm^2), single-labeled bone perimeter (sL.Pm, μm), double-labeled bone perimeter (dL.Pm, μm), and interlabeled width (Ir.L.Wi, μm) were measured. All nomenclature and calculations of the histomorphometric indices are according to Parfitt [51].

2.4 Immunohistochemistry

To better understand the role of caveolin-1 in the growth plate, we characterized the Cav-$1^{-/-}$ phenotype in the costochondral cartilage, proximal tibia, and distal femur of caveolin-1 deficient mice. Mid-sagittal sections of paraffin-embedded tissue (3-5μm)

from the costochondral cartilage and the proximal tibias of 8-week old Cav-$1^{-/-}$ and wild-type mice were stained with haematoxylin and eosin or toluidine blue. Images were examined by microscopy at 10X and 20X. Morphometric measurements were obtained from 10 tibias of 5 animals of each type with the use of Image Pro software (Media Cybernetics; Silver Spring, MD). Measurements included determination of growth plate vertical height (top of resting zone to bottom of calcified cartilage), growth plate width (horizontal plane through the growth plate midsection), and the number of cells in each longitudinal column in the hypertrophic cartilage (the region beginning at the bottom of the proliferating cell zone to the calcified cartilage).

2.5 Transmission Electron Microscopy

Growth zone chondrocytes were cultured in 24-well plates and grown to confluence. The cells were fixed for 1 h at 4°C with 1.6% paraformaldehyde and 3% glutaraldehyde in 0.1 M sodium cacodylate buffer (pH 7.3), washed with 0.1 M sodium cacodylate and 3.5% sucrose buffer (pH 7.3), and then postfixed for 1 h with 1% Palade's OsO_4. Cells were stained en bloc with Kellenberger's uranyl acetate, dehydrated, embedded in epoxy resin, and sectioned [52]. Ultra thin sections were examined with the use of transmission electron microscopy (TEM), and random fields (each field containing part of one or two cells) were photographed. Only distinctly flask-shaped, noncoated vesicles (50–100 nm in diameter) found on the luminal and abluminal plasma membranes were scored as caveolae [53]. Total caveolae counts were normalized to the unit length of plasma membrane measured with the use of Image Pro software (Media Cybernetics; Silver Spring, MD). Caveolae radius was determined by assuming the measured area as circular.

2.6 β-Cyclodextrin Treatment

We used methyl-beta-cyclodextrin (β-CD, Sigma Chemical Company, St. Louis, MO) to deplete lipid rafts of cholesterol and in so doing, alter the caveolar microenvironment. RC and GC cells were treated with β-CD for 30 minutes and then examined by TEM as described above. To assess potential effects of β-CD on caveolin content, confluent cultures were serum starved and then treated with β-CD for 60 min. Cell lysates were examined by Western blot for the presence of caveolin-1, 2 and 3. In addition, rat RC abd GC cells were treated with β-CD for 30 minutes and lysates of the cells were examined for ERp60, VDR and Cav-1 by Western blot. To assess effects of β-CD on rapid $1\alpha,25(OH)_2D_3$-activation of PKC, cells were serum starved for 18 hours in media containing 0.5% FBS. At that time, the cells were treated with medium containing 0.5% lipoprotein-free FBS and β-CD for 30 min. These media were replaced with FBS-free fresh media containing vehicle or 10^{-10} to 10^{-8} M $1\alpha,25(OH)_2D_3$.

2.7 Proteoglycan Sulfation

At confluence, GC cell culture was treated with fresh medium containing vehicle alone, 10^{-8}, and 10^{-9} $1\alpha,25(OH)_2D_3$. Four hours prior to harvest, 50µl DMEM containing 18µCi/ml [^{35}S]-sulfate and 0.814mM carrier sulfate were added to each culture. At harvest, the conditioned media were removed, the cell layers (cells and matrix) collected, and the amount of [^{35}S]-sulfate incorporated determined as a function of cell layer protein.

2.8 Thymidine Incorporation

DNA synthesis was determined by measuring [^{3}H]-thymidine incorporation into trichloroacetic acid (TCA) insoluble cell precipitates as described [54]. Quiescence was

induced by incubating confluent cultures for 48 h in DMEM containing 1% lipoprotein-free FBS. They were then treated for 30 minutes with medium containing 1% lipoprotein-free FBS and β-CD. This medium was replaced with DMEM containing vehicle alone (control), or with either 10^{-10} to 10^{-8} M $1\alpha,25(OH)_2D_3$. At 20 hours, [^{3}H]-thymidine was added and the cells were cultured an additional four hours. Radioactivity in TCA-precipitable material was measured by liquid scintillation spectroscopy.

2.9 Alkaline Phosphatase Activity

To determine if β-CD altered $1\alpha,25(OH)_2D_3$-dependent activation of alkaline phosphatase [orthophosphoric monoester phosphohydrolase, alkaline (EC 3.1.3.1)], following an 18-h incubation in starvation medium containing 0.5% FBS, confluent GC cells were treated for 30-minutes with β-CD in medium containing 0.5% lipoprotein-free FBS. These media were replaced with media containing vehicle or vitamin D metabolite for 24-hours. Alkaline phosphatase specific activity was measured in cell layer lysates as a function of release of *para*-nitrophenol from *para*-nitrophenylphosphate at pH 10.2 [6, 30].

2.10 Protein Kinase C Activity

PKC activity was measured in cell layer lysates prepared by washing the cultures once with cold PBS followed by lysis in 0.3 ml of RIPA buffer (50 mM Tris-HCl, pH 7.5, 150 mM NaCl, 5 mM EDTA, 1 mM phenylmethylsulfonylfluoride, and 1% NP-40 detergent). Aliquots of the cell culture lysates (35 µl) were then incubated for 20 minutes with a lipid preparation (5 µl) containing 0.3 mg/ml phosphatidylserine, 10 µM phorbol-12- Myristate-13-acetate, and Triton X-100 mixed micelles, which provides the necessary cofactors and conditions for optimal activity [15, 16, 55]. To this mixture, a high-affinity

myelin basic protein peptide (MBP, 8 μM) and [^{32}P]ATP (25 μCi/ml) were added to a final assay volume of 50 μl. Following a 10minute incubation in a 30°C waterbath, samples were spotted onto phosphocellulose discs, which were then washed twice with 1% phosphoric acid and once with distilled water to remove unincorporated label prior to placement in a scintillation counter. The phosphocellulose disc strongly binds the MBP peptide substrate, which becomes ^{32}P-labeled during the PKC reaction, and unincorporated [^{32}P]ATP is washed free of the discs during the phosphoric acid wash step [55].

2.11 Western Blot

Protein samples were resolved on 4-20% gradient Tris-HCl Ready Gel (161-1159; Biorad, Hercules, CA) at 80V for 15 min and 120 V thereafter. Wet transfer was performed for 2 hours at 80V in a transfer case onto nitrocellulose membrane (Biorad). The membrane is blocked with 5% nonfat dry milk in PBS-Tween solution. Blots of the gels were probed with mouse monoclonal antibodies to caveolin-1 (Ab2297: anti-RSV-CEF caveolin) [56], caveolin-2 (m65: anti-human caveolin-2) [57], caveolin-3 (m26: anti-rat caveolin-3) [58] (Transduction Laboratories, Lexington; KY), ERp60 (Ab100 generated to the N-terminal amino acid sequence of rat ERp60), and VDR (C-20: Santa Cruz Biotechnology, Santa Cruz, CA). All antibodies were used at 1:500 dilution in nonfat dry milk in PBS-Tween. The membrane is subsequently washed with PBS-Tween three times at 10min each. Goat anti-mouse or anti-rabbit secondary HRP with a dilution of 1:5000 in PBS-Tween is added to the membrane for one hour. Repeat wash with PBS-Tween. West Pico Chemiluminescent ECL substrate (34080; Pierce, Rockford, IL) is used for detection of HRP. VersaDoc (Biorad) is used to image the membrane.

2.12 Immunocytochemistry

Chondrocytes were cultured on multi-well chamber slides (Nunc Lab-Tek II CC2 Chamber Slide System) for 24 hours, partially permeabilized for 20 min with 3.7% (v/v) formaldehyde at room temperature, and permeabilized with ice-cold ethanol for 5 min according to conventional protocols [38]. Cells were then incubated with 5% bovine serum albumin (BSA) at room temperature for 1 hour to reduce background staining, and treated with primary antibodies against VDR (C-20: Santa Cruz Biotechnology, Santa Cruz, CA), ERp60 (Ab100 generated to the N-terminal amino acid sequence of rat ERp60), and caveolin-1 (Ab2297: Transduction Laboratories, Lexington; KY) at room temperature for 2 hours. Cells were then treated with secondary FITC- and rhodamine-conjugated anti-rabbit and anti-mouse antibodies, respectively (Santa Cruz Biotechnology, CA) in a 1:200 dilution for 2 hours. Samples were visualized with a laser scanning confocal Zeiss LSM 510 microscope (Carl Zeiss, Inc.) using a 63x immersion lens with aperture and PBS buffer as the imaging medium. Zeiss confocal software was used for acquisition of the data and merging of the digital images. Controls were performed with no primary antibody.

Immunofluorescent labeling of lipid rafts was performed using the Vybrant Lipid Raft Labeling Kit (V-34403 Vybrant Alexa Fluor 488: Molecular Probes, Carlsbad; CA). Slides were washed with chilled DMEM. Fluorescent choleratoxin subunit-B (CT-B) conjugate working solution was added to the cells for 10 minutes at 4^{o}C. After incubation, cells were washed several times with chilled 1X PBS. The cells were then introduced to chilled anti-CT-B antibody working solution for 15 minutes at 4^{o}C,

followed by washing several times with chilled 1X PBS. Cells were then fixed with formaldehyde as described above and probed with the appropriate antibodies.

2.13 Plasma Membrane and Extracellular Matrix Vesicle Isolation

Cells were cultured in T75 flasks until confluent. The cell layers were washed twice with 3 mL DMEM. Trypsin (0.25%; 3mL) was added to each flask until cells detached from flask surface. After sufficient incubation, DMEM containing 10% FBS was added to each flask to deactivate the trypsin. After centrifugation for 10 minutes at 500 x g, the supernatant was collected and used to obtain matrix vesicles while the pellet was used to isolate plasma membranes. To isolate matrix vesicles, the supernatant was spun at 17500 x g for 20min (rotor SA600; Beckman Coulter, Fullerton, CA) to pellet large cell fragments and membranes. The resulting supernatant was re-spun at 85,000 x g for 60min at 4^{o}C (rotor 50.2 Ti, Beckman Coulter). After discarding the supernatant, the pellet was suspended with 20 mL 0.9% NaCl and spun again at 85,000 x g for 60min. The resultant pellet was resuspended with 0.5 mL 0.9% NaCl and stored at -20^{o}C. For plasma membrane isolation, the cell pellet was resuspended in 5 mL 0.25 M sucrose containing 1 mM EDTA and 100 mM Tris in ultrapure water, pH 7.4. The sample was homogenized with a Tenbroek tissue homogenizer. The homogenate was centrifuged at 1464 x g for 10 min (rotor SA 600), and the pellet suspended in 5 mL 2M sucrose in ultrapure water. Following centrifugation at 200 x g for 10 minutes, the resulting supernatant was brought to 35 mL using ice-cold ultrapure water and centrifuged at 28000 x g for 15 min. The final pellet was resuspended in 1 mL 0.9% NaCl and stored at -20^{o}C.

2.14 Lipid Raft/Caveolae Fractionation

Lipid rafts/caveolae fractionation was adapted from Smart et al. [33]. Chondrocytes were grown to confluence in six T-75 flasks. The cells were washed twice with ice cold PBS and then washed twice with buffer A (0.25M sucrose, 1 mM EDTA, 20 mM Tricine, pH 7.8). Each flask is scraped with 3ml of buffer A. Samples of the resulting suspension was taken and sonicated to use as whole cell homogenates. The rest of the suspension was centrifuged for 5 min at 1400 x g to pellet the cells. The pellet was resuspended in 1 ml of buffer A and homogenized with 2 ml Wheaton Tissue Grinder (Wheaton Science; Millville, NJ). The suspension was then centrifuged at 1000 x g for 10 min and the supernatant, containing the post-nuclear sample (PNS), was removed and stored on ice. The remaining pellet was re-suspended in 1 ml buffer A and re-homogenized and centrifuged at 1000 x g for 10 min. The resulting supernatant was added to the previous PNS. The remaining pellet was re-suspended in 1 ml buffer A and stored as nuclear fraction (NF) after sonication. The remaining PNS was layered carefully using a glass pipette tip on top of 8 ml of 30% v/v Percoll (Sigma; St. Louis, MO) in buffer A. Samples were centrifuged at 84,000 x g for 30 min using a Beckman SW 41 Ti rotor. Plasma membranes form a visible band in the middle of the centrifuge tube. The membrane fraction was collected using a syringe with a bent needle and then sonicated (2 × 15-s bursts at power level 4, total of 10 times; Fisher Scientific Sonic Dismembrator 60). The samples were adjusted to 4 ml with 1.84 ml buffer C (50% Opti-Prep in buffer B) (buffer B: 0.25 M sucrose, 6 mM EDTA, 120 mM Tricine, pH 7.8) for an OptiPrep (Greiner-Bio-one, Longwood, FL) concentration of 23%. The samples were placed at the bottom of a centrifuge tube (Beckman-Coulter) and overlaid with a linear gradient of 20% to 10% OptiPrep in buffer A. The samples were centrifuged 24 h at

52,000 × g and the top 5 ml was collected. The 5-ml samples were mixed with 4 ml of buffer C in a fresh centrifuge tube and overlaid with 5% OptiPrep in buffer A then centrifuged again for 20 h at 52,000 × g. Fractions were collected (0.73 ml) and numbered 1 to 12 from the top. The fractions were saved and the protein concentration determined for analysis by Western blot.

2.15 Statistical Management of Data

For each experiment, the values represent mean ± SEM for cell layers in six independent cultures. Significance was determined by using ANOVA and post-hoc testing performed using Bonferroni's modification of Student's *t*-test. P-values less than 0.5 were considered significant. Each experiment was repeated two to three times to ensure validity of the results.

CHAPTER 3. RESULTS

3.1 Physiological Importance

Static and dynamic morphometric histomorphometry of mice injected with calcein at 6 and 2 days prior to euthanasia at 8.5 weeks demonstrated physiological differences between cav-$1^{+/+}$ and cav-$1^{-/-}$ mice (Table 1). While the trabecular bone did not show significant changes in trabecular number and trabecular width, the total trabecular bone volume (TV) and the trabecular fraction (BV/TV) increased from 77,408±7,211 μm^2 to 114,042±9,434 μm^2 and 21.4±2.0% to 31.5±2.6%, respectively ($p \leq 0.05$). Dynamic trabecular bone morphometrics showed that the trabecular mineral apposition rate (MAR) decreased by 41% and bone formation rate (BFR) decreased by 47.7% in cav-$1^{-/-}$ mice. The MAR of the cortical bone also showed a significant decrease of 67.8% ($p \leq 0.05$).

Histologic analysis demonstrated that the physiology of the tissue was altered by Cav-1 deficiency. Tibial (Fig. 5) growth plates of 8-week-old wild type mice exhibited normal remodeling of the calcified cartilage. As shown in Fig 5A and 5B, the tibial growth plate in wild type mice was relatively acellular, and epiphyseal and metaphyseal bone surrounded well-developed marrow. The tibial growth plates of the Cav-$1^{-/-}$ mice were longer and cartilage extended into the epiphyseal bone and metaphyseal marrow (Fig 5C and 5D). In the metaphysis, these trabeculae were coated with a thin layer of bone. Morphometric analysis of the histologic sections showed that Cav-$1^{-/-}$ tibial growth plates were 12.3 % longer than those of wild type mice (Fig. 5). The number of columns of cells in the proliferating cell zone and in the hypertrophic cell zone was greater in Cav-$1^{-/-}$ growth plates. In addition, for each column of cells, the number of hypertrophic cells

Table 1. Dynamic Morphometry

A. TRABECULAR BONE

i. Static Morphometrics

	cav-1$^{(+/+)}$		cav-1$^{(-/-)}$		cav-1$^{(-/-)}$ /cav-1$^{+/+)}$
	Mean	SEM	Mean	SEM	
Total Trabecular Bone Volume (TV) μm^2	77,408	7,211	114,042 *	9,434	
BV/TV %	21.35	1.99	31.45 *	2.6	147.3
Trabecular #	11	0.84	12.8	0.49	
Trabecular Width (Tb.Th) μm	215.14	8.77	200.76	26.83	

ii. Dynamic Trabecular Bone Morphometrics

	cav-1$^{(+/+)}$		cav-1$^{(-/-)}$		cav-1$^{(-/-)}$ /cav-1$^{+/+)}$
	Mean	SEM	Mean	SEM	
MAR μm/day	2.93	0.41	1.73 *	0.13	59.04
BFR μm%/day	1.49	0.26	0.78 *	0.07	52.35

B. CORTICAL BONE: Dynamic Cortical Bone Morphometrics

	cav-1$^{(+/+)}$		cav-1$^{(-/-)}$		cav-1$^{(-/-)}$ /cav-1$^{+/+)}$
	Mean	SEM	Mean	SEM	
MAR μm/day	4.94	0.29	1.59 *	0.4	32.19

* Significant difference compared to cav-1$^{(+/+)}$

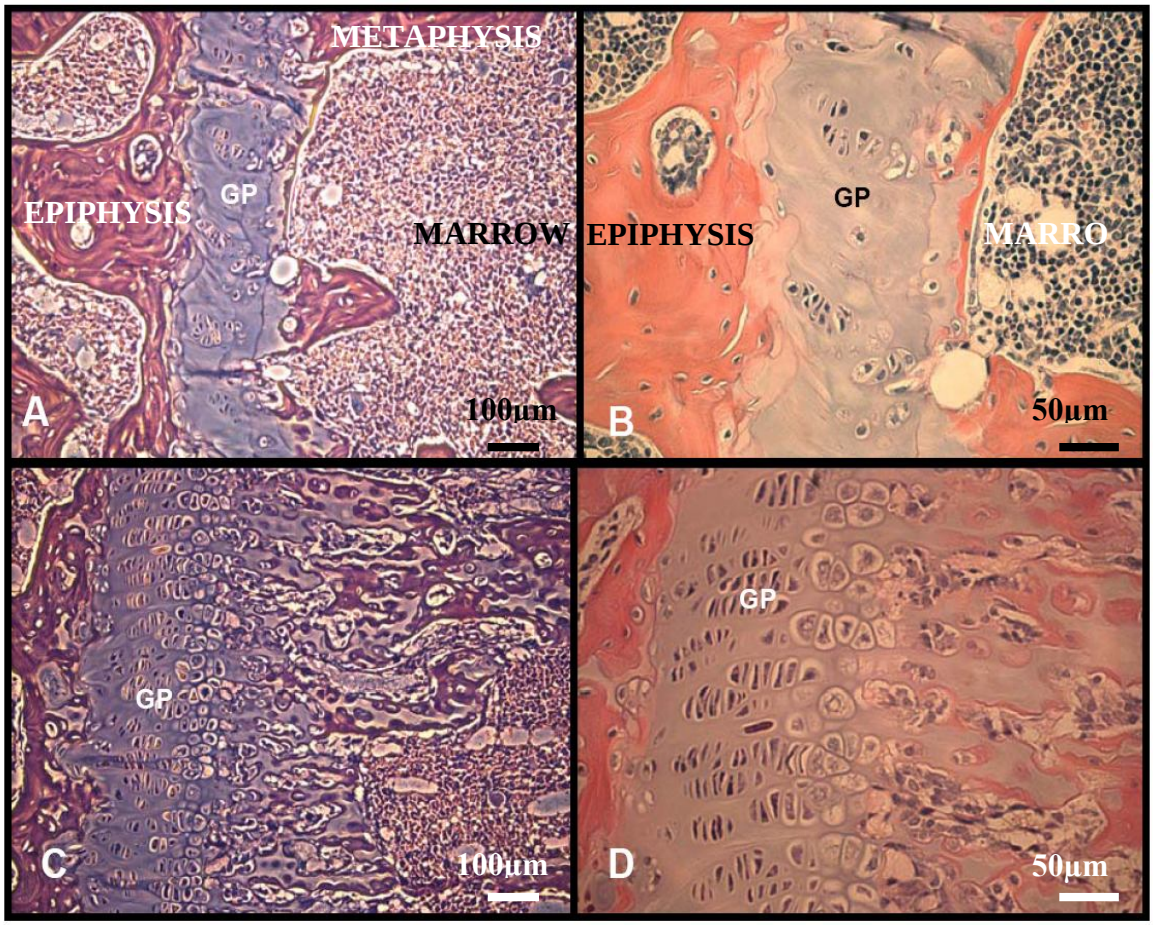

Mice	Growth Plate Height (µm)	Growth Plate Width (µm)	Number of Hypertrophic Cells/Column	Number of Proliferative Cells/Column
Wild Type	121.3±3.7	1729±82	4.19±0.2	10.0±0.3
Cav-1$^{-/-}$	136.2±5.0*	1982±52	6.23±0.3*	10.1±0.8

Figure 5. H&E stained histologic sections of the tibial growth plates of wild-type mice and Cav-1$^{-/-}$ mice. Sections were photographed at 10X and 20X magnification: wild-type growth plate at 10X magnification (A) and 20X magnification (B); Cav-1$^{-/-}$ growth plate at 10X (C) and at 20X (D). The bars indicate the final magnification. Sections are oriented with epiphysis on the left and metaphysic on the right.

* Significant difference compared to wild type

were greater in Cav-$1^{-/-}$ growth plates than in wild-type growth plates, although the number of proliferating cells per column was comparable. RC cartilage in tibial growth plates of Cav-$1^{-/-}$ and wild-type animals was relatively small, although there was evidence of a residual resting zone in Cav-$1^{-/-}$ limbs, characterized by chondrocytes that were not aligned in columns and had not yet begun the proliferative process.

3.2 Cellular Importance

Transmission electron microscopy demonstrated the presence of intact caveolae in RC and GC cells in vitro and in vivo (Fig. 6). Morphometric analysis were performed with the in vitro samples due to difficulties with observing plasma membrane associated caveole because of large numbers of cytoplasmic extensions into the extracellular matrix. Analysis show cellular specificity in caveolae number and size (Table 2). GC cells had 3.7 times more caveolae/100 μm plasma membrane than RC cells. GC caveolae were more spherical in shape, with comparable long and short axes. Caveolae in RC cells were more oval in shape; their short axis was comparable to that measured in GC cells, but the long axis was approximately 20% longer, resulting in a small but statistically significant difference in the average radius and a 24.4% increase in cross-sectional area.

Western blot analysis showed that rat RC and GC cells had comparable levels of caveolin-1, -2 and -3 (Fig. 7). Treatment of rat growth zone chondrocytes with β-CD altered the response of the cells to $1\alpha,25(OH)_2D_3$. The rapid stimulatory effect of $1\alpha,25(OH)_2D_3$ on PKC was reduced in a dose-dependent manner (Fig 8A). β-CD had no affect on PKC activity in control cultures, but 1 mM β-CD partially reduced the stimulatory effect of 10^{-8} M $1\alpha,25(OH)_2D_3$ and 5 mM β-CD completely abrogated the $1\alpha,25(OH)_2D_3$-dependent increase in PKC. This dose-dependent effect of β-CD was

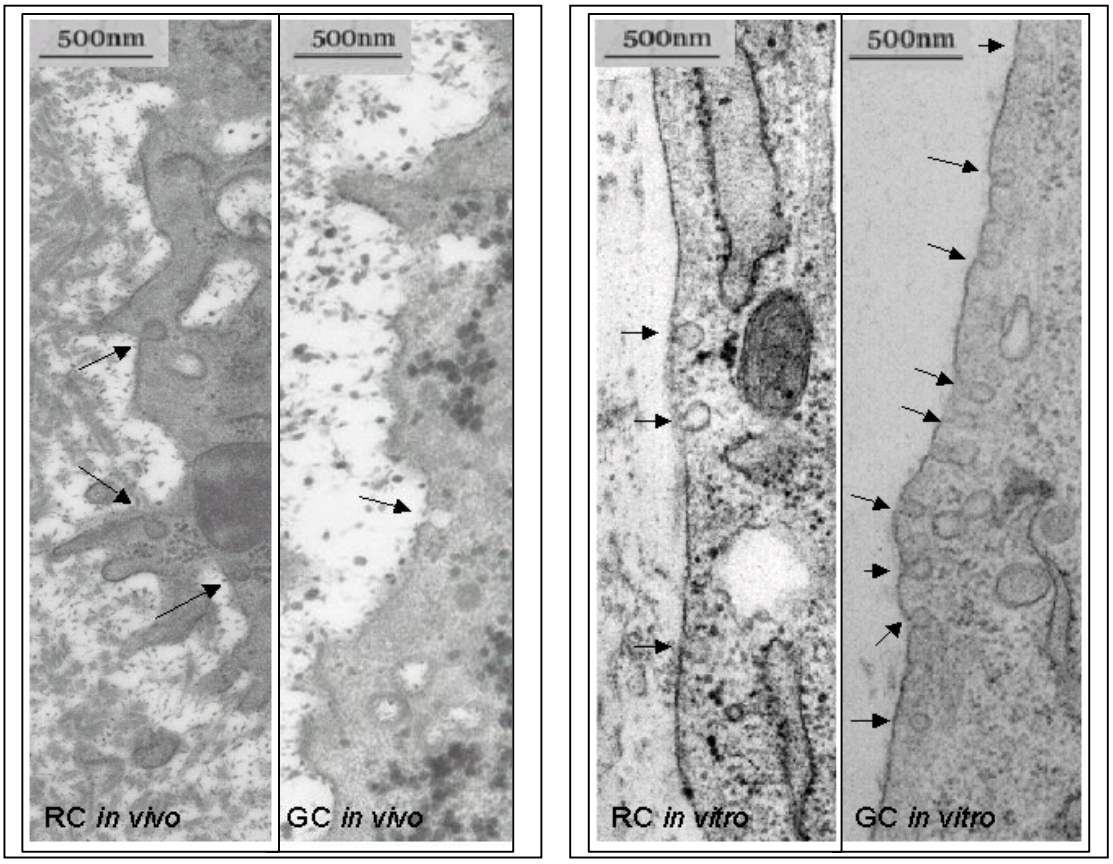

Figure 6. TEMs of caveolae associated with the plasma membranes of rat costochondral resting zone (RC) and growth zone (GC) chondrocytes in vivo (left) and in vitro (right). Bar=500nm. Arrows point to caveolae.

Table 2. Morphometric Analysis

	Open Caveolae /100mm PM	Closed Caveolae /100mm PM	Total Caveolae /100mm PM	Long Diameter (mm)
GC (n=55)	12.8±2.6	2.4±0.6	15.3±2.9	58.45±0.61
RC (n=39)	3.6±0.8*	0.4±0.2*	4.1±.8*	69.97±3.88*
GC/RC	3.6	6.0	3.7	0.8
	Short Diameter (mm)	Caveolar Area (mm2)	Caveolar Radius (mm)	
GC (n=55)	58.28±0.93	3545.8± 71.3	33.35±0.37	
RC (n=39)	58.56±2.74	4410.7±392.6*	36.37±1.69*	
GC/RC	1.0	0.8	0.9	

PM: Plasma Membrane

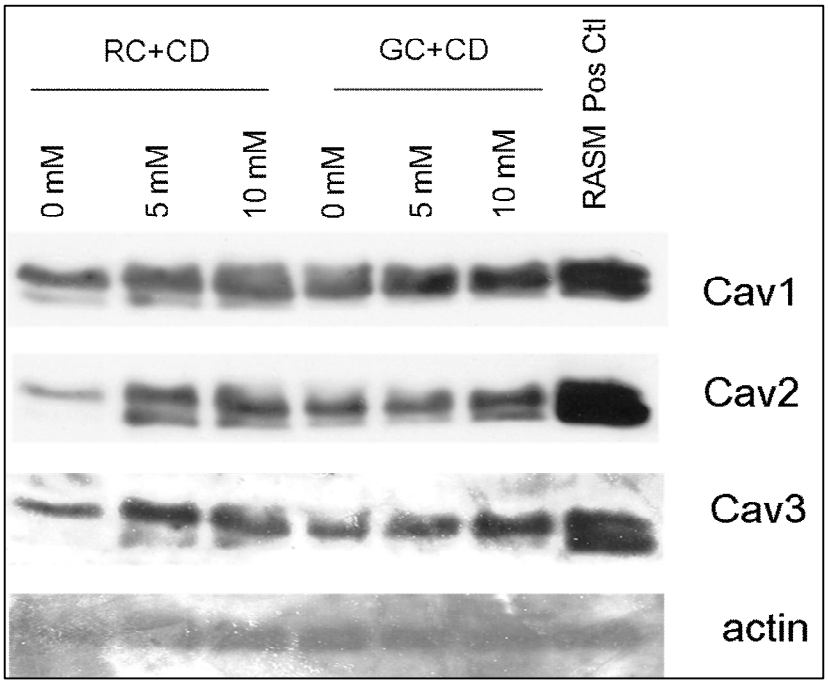

Figure 7. Caveolin proteins in lysates of rat costochondral resting zone (RC) and growth zone (GC) chondrocytes. Confluent cultures of RC and GC cells were treated for 60 minutes with 0, 5 or 10 mM β-CD (CD). Cultures were lysed and Western blots of the lysates were probed with antibodies to Cav-1, Cav-2 and Cav-3. Rat arterial smooth muscle cells (RASM) were used as positive controls and actin was used as an internal loading control.

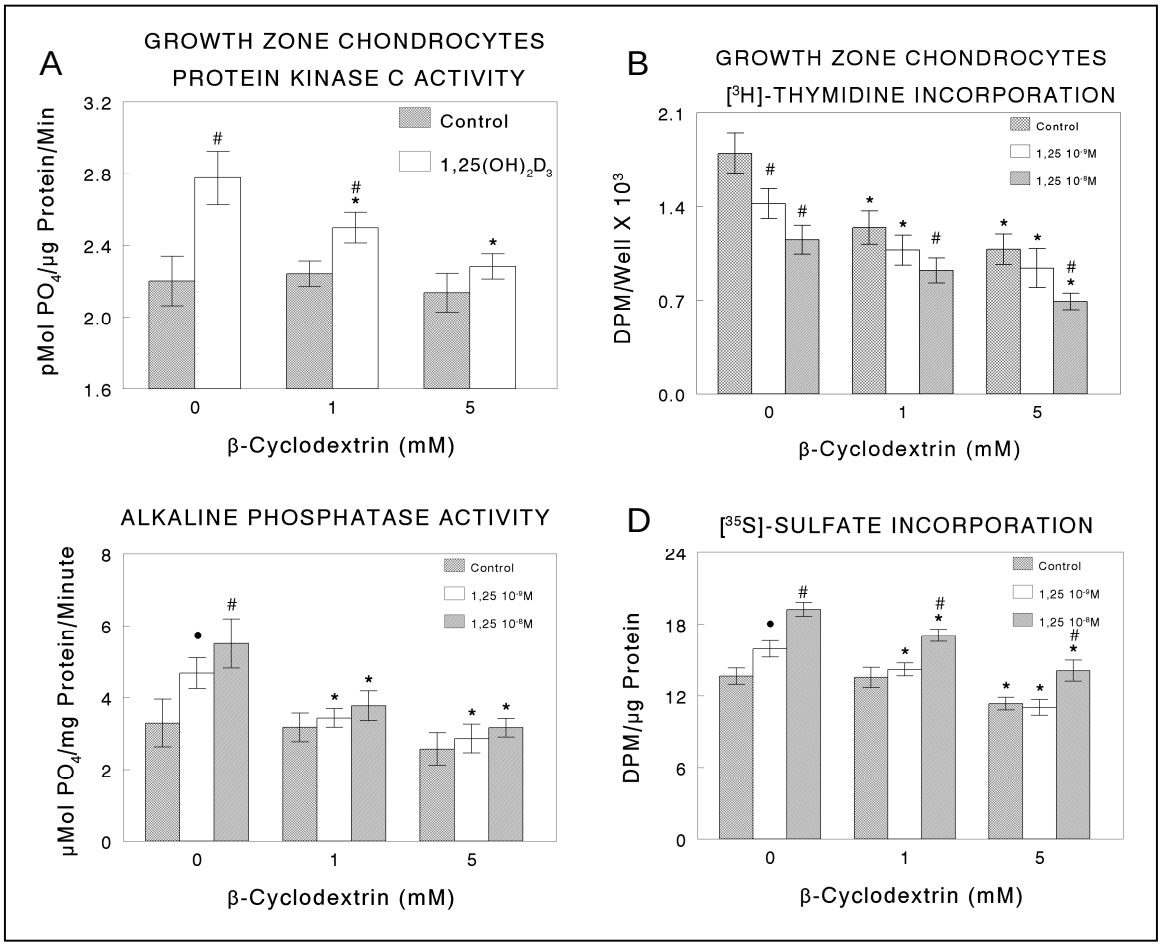

Figure 8. Effect of β-CD treatment on biological responses of rat costochondral growth zone chondrocytes to $1\alpha,25(OH)_2D_3$. GC cells were pretreated with β-CD for 30 minutes followed by treatment with 0 or 10-8 M $1\alpha,25(OH)_2D_3$ for 9 minutes and PKC specific activity determined (A). To assess the effects of β-CD on DNA synthesis, preconfluent cultures were treated for 30 minutes with 0, 1 or 5 mM β-CD followed by treatment with 0, 10^{-9} or 10^{-8} M $1\alpha,25(OH)_2D_3$ for 24 hours and [^{3}H]-thymidine incorporation measured (B). Alkaline phosphatase specific activity (C) and [^{35}S]-sulfate incorporation (D) were determined in confluent cultures treated with β-CD for 30 minutes followed by treatment with $1\alpha,25(OH)_2D_3$ for 24 hours. Data are from one of two separate sets of experiments, both with comparable results. Values are means $\pm$ SEM for six independent cultures. *$p<0.05$, with β-CD v. without β-CD at each concentration of $1\alpha,25(OH)_2D_3$. #$p<0.05$, with $1\alpha,25(OH)_2D_3$ v. without $1\alpha,25(OH)_2D_3$ at each concentration of β-CD. ●$p<0.05$, with 10^{-9} M $1\alpha,25(OH)_2D_3$ v. no $1\alpha,25(OH)_2D_3$ in the absence of β-CD.

observed in five separate experiments based on comparative analysis of treatment/control ratios for each experiment (data not shown). β-CD also blocked long term downstream effects of 1α,25$(OH)_2D_3$ on DNA synthesis (Fig. 8B) and alkaline phosphatase specific activity (Fig. 8C). In addition, β-CD caused a partial inhibition in the effect of 1α,25$(OH)_2D_3$ on [^{35}S]-sulfate incorporation (Fig 8D). When rat RC and GC cells were treated with β-CD to deplete lipid rafts/caveolae of cholesterol, the number of caveolae was reduced in each cell type (Fig. 9). This was evident in TEMs of the cells and was confirmed by morphometric analysis of the number of caveolae per 100 μm of plasma membrane. Although the number of caveolae was reduced, there was no apparent reduction in the levels of Cav-1, Cav-2 or Cav-3 (Fig. 7) or in the levels of ERp60 and VDR (Fig. 10 and Fig. 11).

While β-CD is a useful reagent to initially probe whether lipid rafts/caveolae are involved in response to humoral and mechanical stimuli, it does not provide sufficient direct evidence for their roles. Therefore, we used Cav-$1^{-/-}$ mice to determine whether Cav-1 and caveolae are involved in 1α,25$(OH)_2D_3$ action in the growth plate. GC cells obtained from Cav-$1^{-/-}$ mice failed to exhibit a response to 1α,25$(OH)_2D_3$. There was no change in PKC specific activity (Fig. 12A), alkaline phosphatase specific activity (Fig. 12B) or [^{35}S]-sulfate incorporation (Fig. 12C), when Cav-$1^{-/-}$ mice were treated with 1α,25$(OH)_2D_3$. In contrast, GC cells from wild-type animals exhibited anticipated increases in PKC (Fig. 12A), alkaline phosphatase (Fig. 12B) and [^{35}S]-sulfate incorporation (Fig. 12C). Transmission electron microscopy of RC cells confirmed that

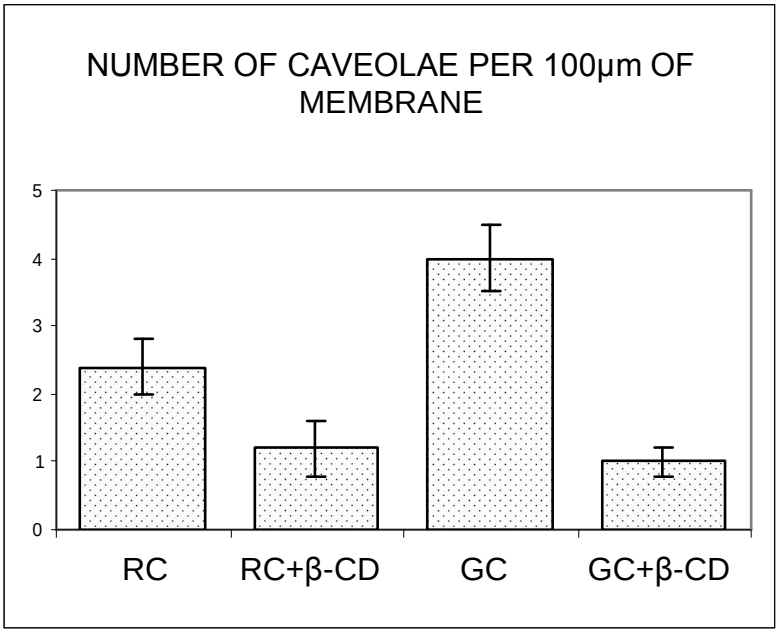

Figure 9. Morphometric assessment shows that GC cells have more caveolae than RC cells and that β-CD treatment significantly decreased the number of caveolae in both cell types. Data are means $\pm$ SEM for 20 cells of each type.

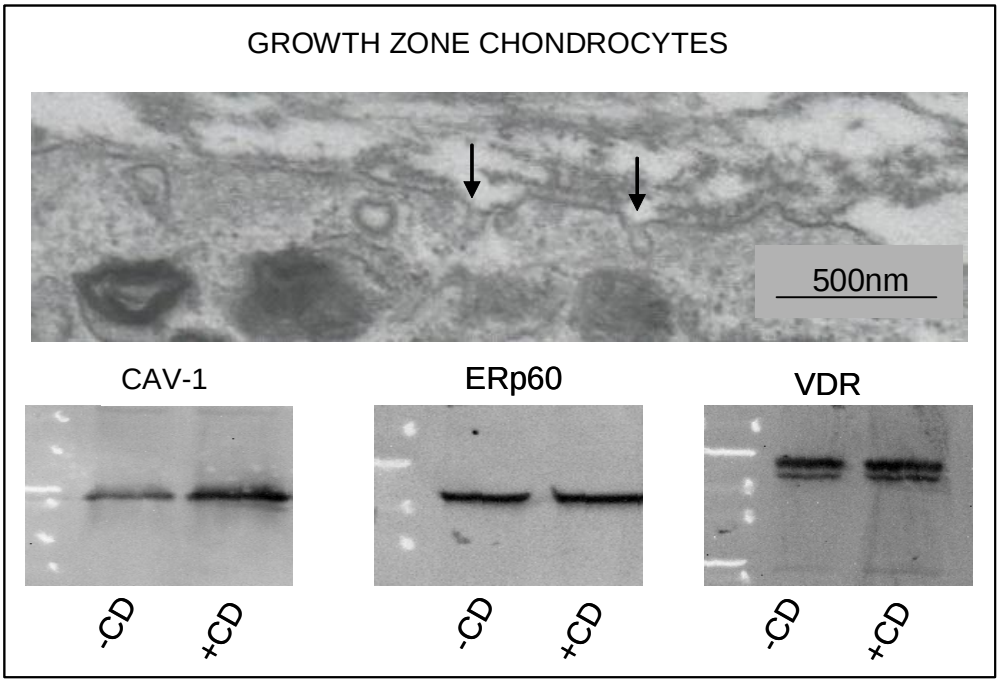

Figure 10. Effects of β-CD treatment on confluent cultures of GC cells. TEM of GC chondrocytes demonstrates the presence of caveolae (arrows) in the treated cells. Western blots of GC cell lysates indicate that the amount of Cav-1, ERp60 and VDR in the cells were not affected by β-CD treatment.

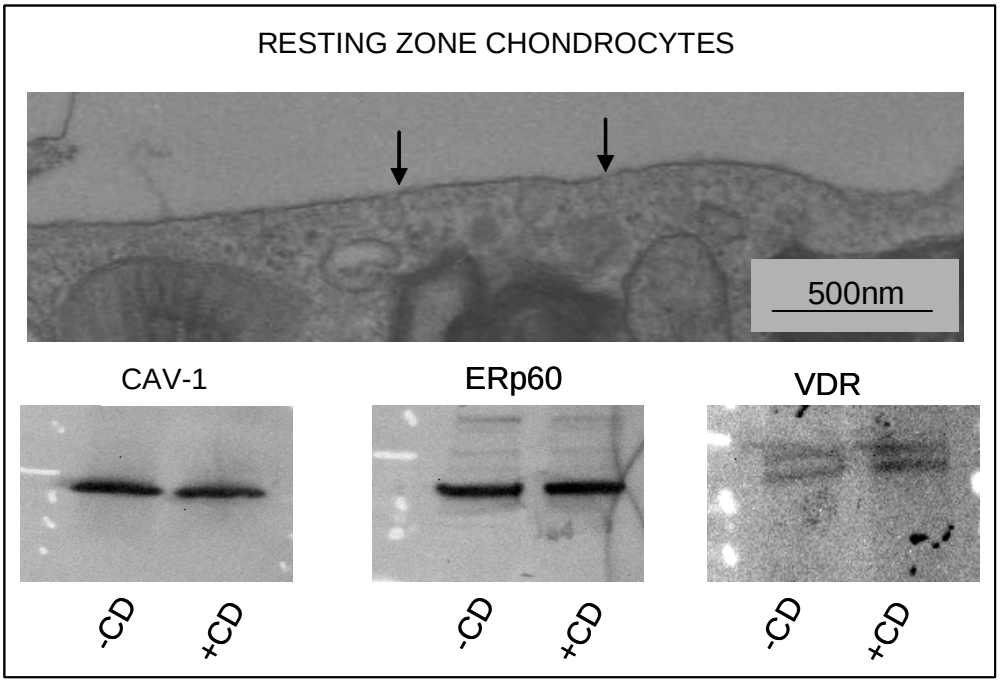

Figure 11. Effects of β-CD treatment on confluent cultures of RC cells. TEM of RC chondrocytes demonstrates the presence of caveolae (arrows) in the treated cells. Western blots of RC cell lysates indicate that the amount of Cav-1, ERp60 and VDR in the cells were not affected by β-CD treatment.

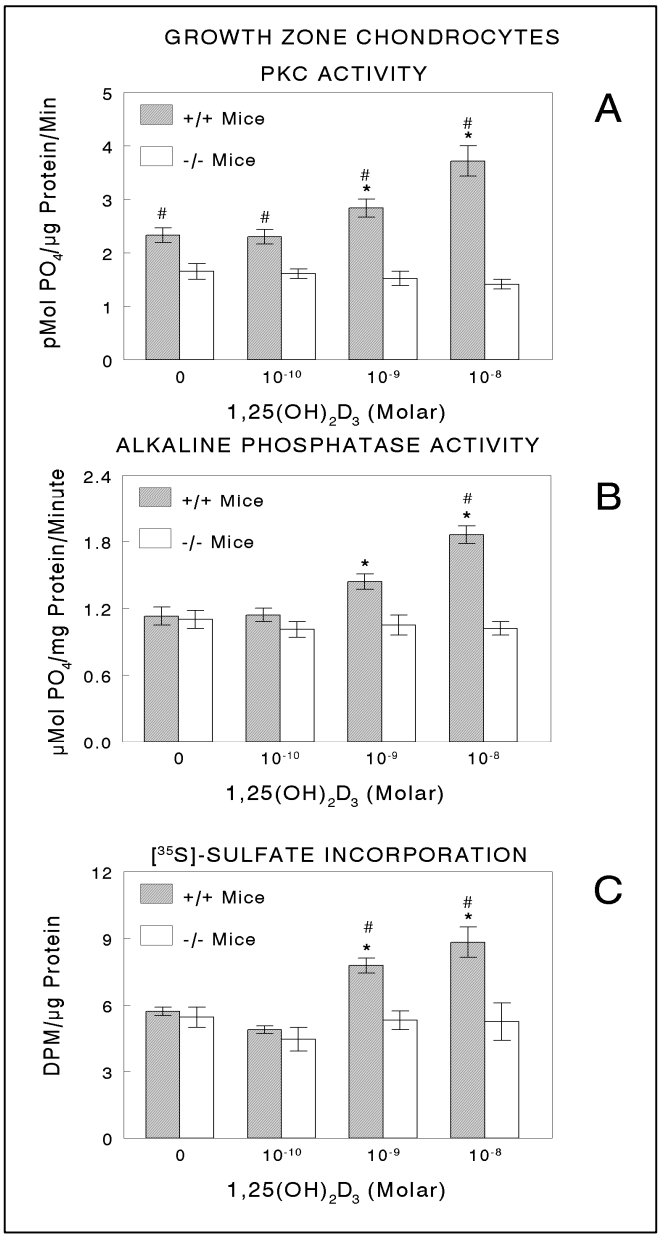

Figure 12. Response of Cav-$1^{-/-}$ and wild-type (Cav-$1^{+/+}$) mouse GC chondrocytes to $1\alpha,25(OH)_2D_3$. Effects on PKC (A), alkaline phosphatase (B), and [^{35}S]-sulfate incorporation (C) were determined. Data are from one of two separate sets of experiments, both with comparable results. Values are means $\pm$ SEM for six independent cultures. *$p<0.05$, with β-CD v. without β-CD at each concentration of $1\alpha,25(OH)_2D_3$. #$p<0.05$, with $1\alpha,25(OH)_2D_3$ v. without $1\alpha,25(OH)_2D_3$ at each concentration of β-CD. TEM of Cav-$1^{-/-}$ mouse resting zone cells showing absence of caveolae. Western blot showing the absence of Cav-1 in lysates of Cav-$1^{-/-}$ resting zone chondrocytes and the presence of Cav-1 in lysates of chondrocytes from wild type C57BL/6 mice.

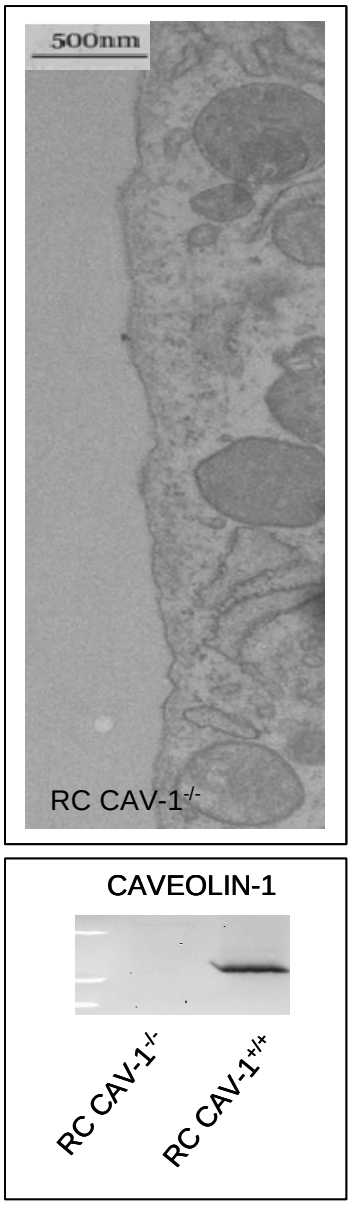

Figure 13. TEM of Cav-$1^{-/-}$ mouse resting zone cells showing absence of caveolae. Western blot showing the absence of Cav-1 in lysates of Cav-$1^{-/-}$ resting zone chondrocytes and the presence of Cav-1 in lysates of chondrocytes from wild type C57BL/6 mice.

Cav-$1^{-/-}$ chondrocytes lacked caveolae and Western blots of RC cell lysates demonstrated that Cav-1 was absent (Fig. 13).

3.3 Cellular Localization

Confocal microscopy of growth zone chondrocytes show that nVDR is localized in the nuclear region while ERp60 is localized in the perinuclear regions (Fig. 14). In growth zone chondrocytes, ERp60 co-localized with caveolin-1 in the peri-nuclear region and plasma membrane (Fig. 15). In contrast, VDR was found primarily in the nucleus and did not co-localize with caveolin-1 (Fig. 15). Similarly, only ERp60 co-localized with lipid rafts (Fig. 16). Confocal microscopy of resting zone chondrocytes also show localization of caveolin-1 with ERp60 but not VDR (Fig. 17). Co-localization of ERp60 with lipid rafts was also confirmed (Fig. 18). Western blots of GC cell lysates, plasma membranes, and matrix vesicles confirmed that Cav-1 and ERp60 were present in cell lysates and isolated plasma membranes, whereas VDR was present only in the cell lysates of the growth zone cells (Fig. 19). Similar results were also found in RC cells (Fig. 20). Confocal microscopy of $VDR^{-/-}$ GC cells demonstrated that in the absence of VDR, there were co-localization of ERp60 with Cav-1 (Fig. 21). Further western analysis of RC cells from wild-type, Cav-$1^{-/-}$, and $VDR^{-/-}$ mice show the presence of ERp60 despite the absence of Cav-1 and VDR (Fig. 22). Additionally, in growth zone chondrocytes of Cav-$1^{-/-}$ mice, while there was a noticeable lack of Cav-1 immunofluorescent staining and VDR localization with lipid rafts, there was also a lack of co-localization between ERp60 and lipid rafts (Fig. 23). Western analysis of caveolae/lipid raft fractions further indicated the localization of proteins involved in $1\alpha,25(OH)_2D_3$ signaling. In both GC

and RC cells, both ERp60 and PLAA were shown to co-fractionate with Cav-1 (Fig. 24 and 25).

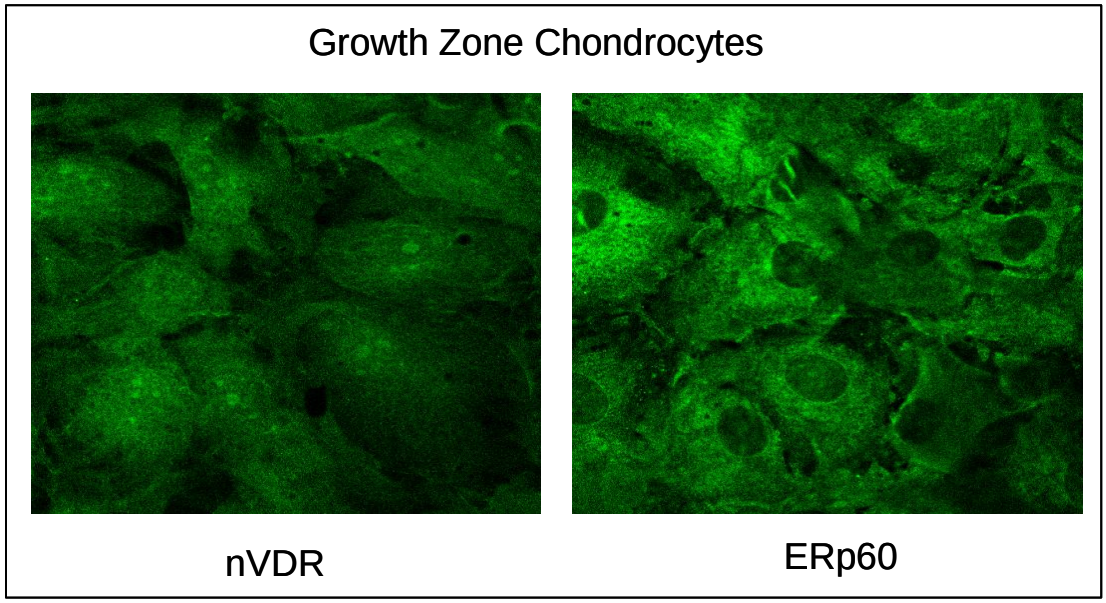

Figure 14. Laser scanning confocal microscopy of rat GC chondrocytes demonstrating subcellular localization of nuclear VDR and ERp60. Result was found in over 50% of the cells examined.

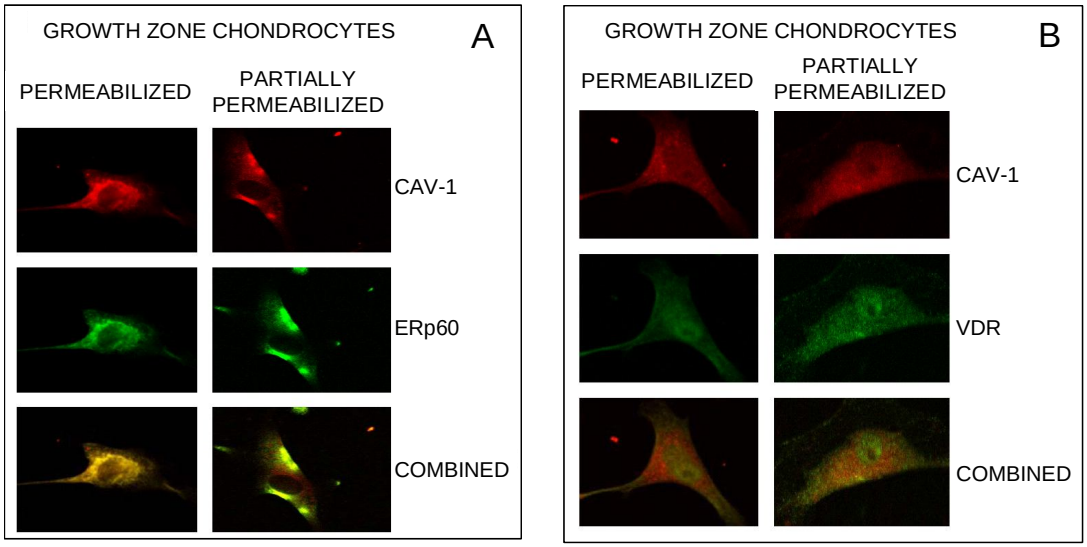

Figure 15. Laser scanning confocal microscopy of rat GC chondrocytes demonstrating subcellular localization of caveolin-1 and ERp60 (A) or caveolin-1 and the nuclear VDR (B). Result was found in over 50% of the cells examined.

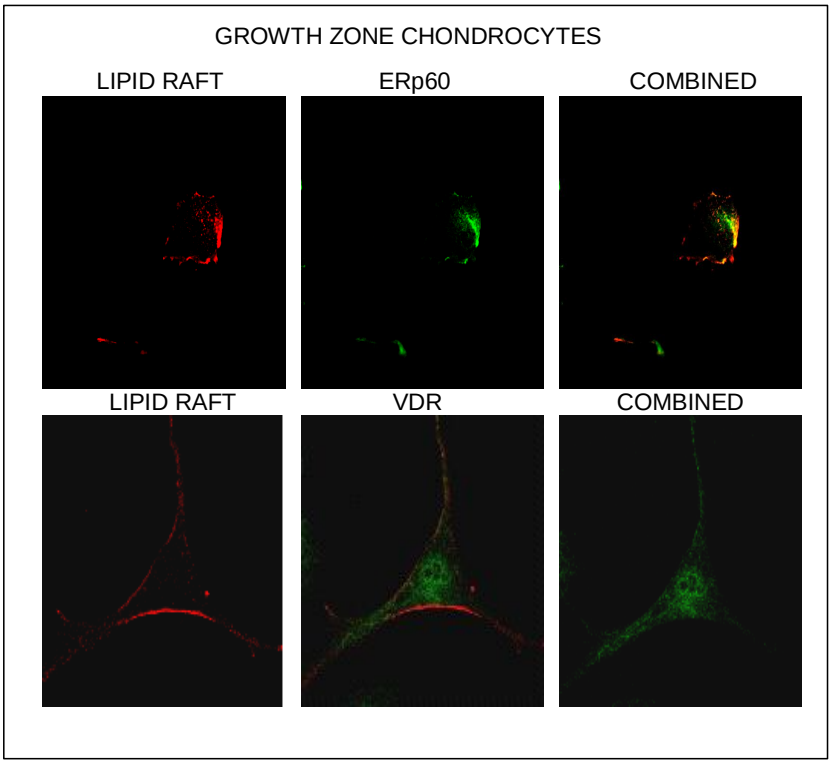

Figure 16 Laser scanning confocal microscopy of rat GC chondrocytes demonstrating subcellular localization of lipid rafts and ERp60 or caveolin-1 and nuclear VDR. Result was found in over 50% of the cells examined.

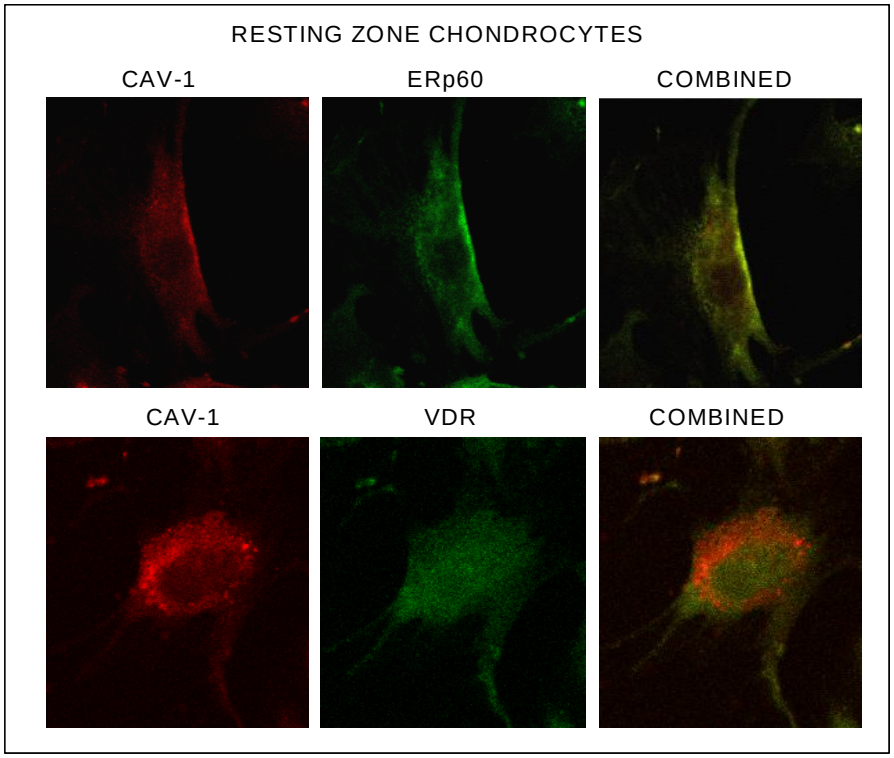

Figure 17. Laser scanning confocal microscopy of rat RC chondrocytes demonstrating subcellular localization of caveolin-1 and ERp60 or caveolin-1 and nuclear VDR. Result was found in over 50% of the cells examined.

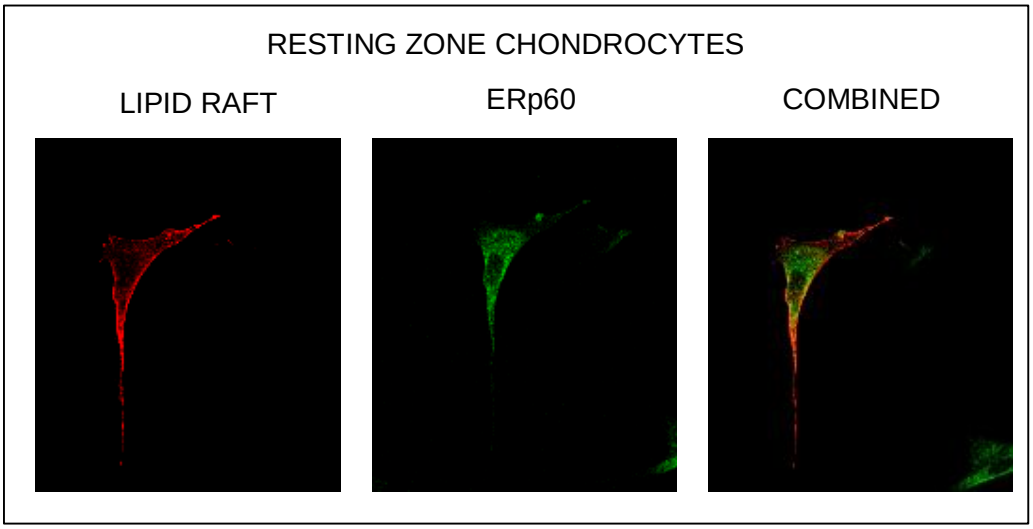

Figure 18. Laser scanning confocal microscopy of rat RC chondrocytes demonstrating subcellular localization of caveolin-1 and ERp60. Result was found in over 50% of the cells examined.

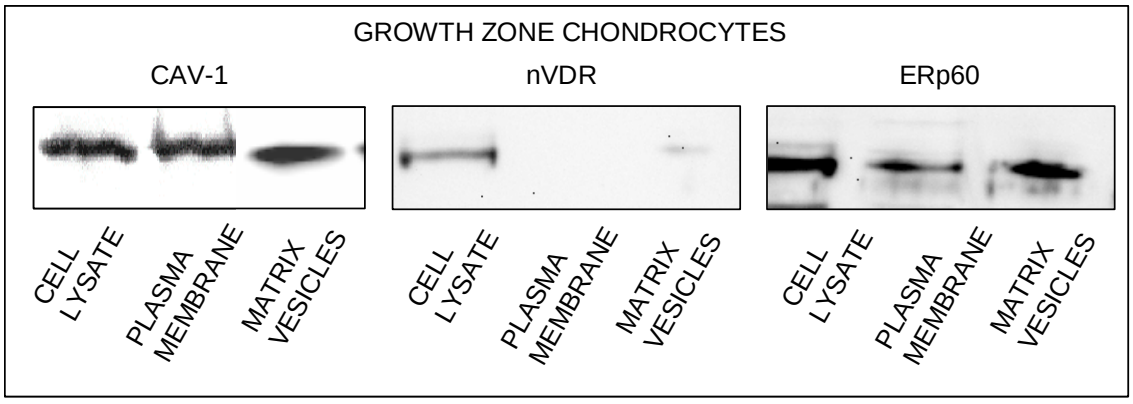

Figure 19. Western blot showing the localization of caveolin-1, VDR, and ERp60 in GC cells using cell lysate, plasma membrane fractions, and matrix vesicles.

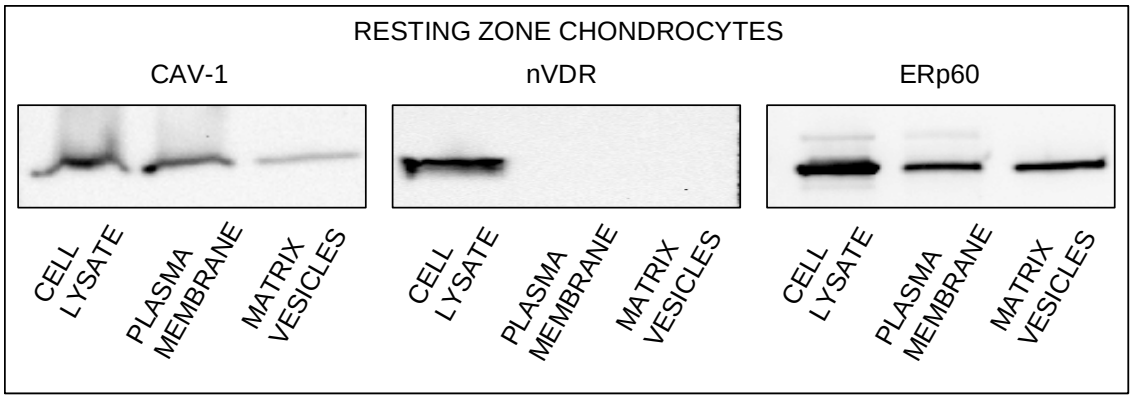

Figure 20. Western blot showing the localization of caveolin-1, VDR, and ERp60 in RC cells using cell lysate, plasma membrane fractions, and matrix vesicles.

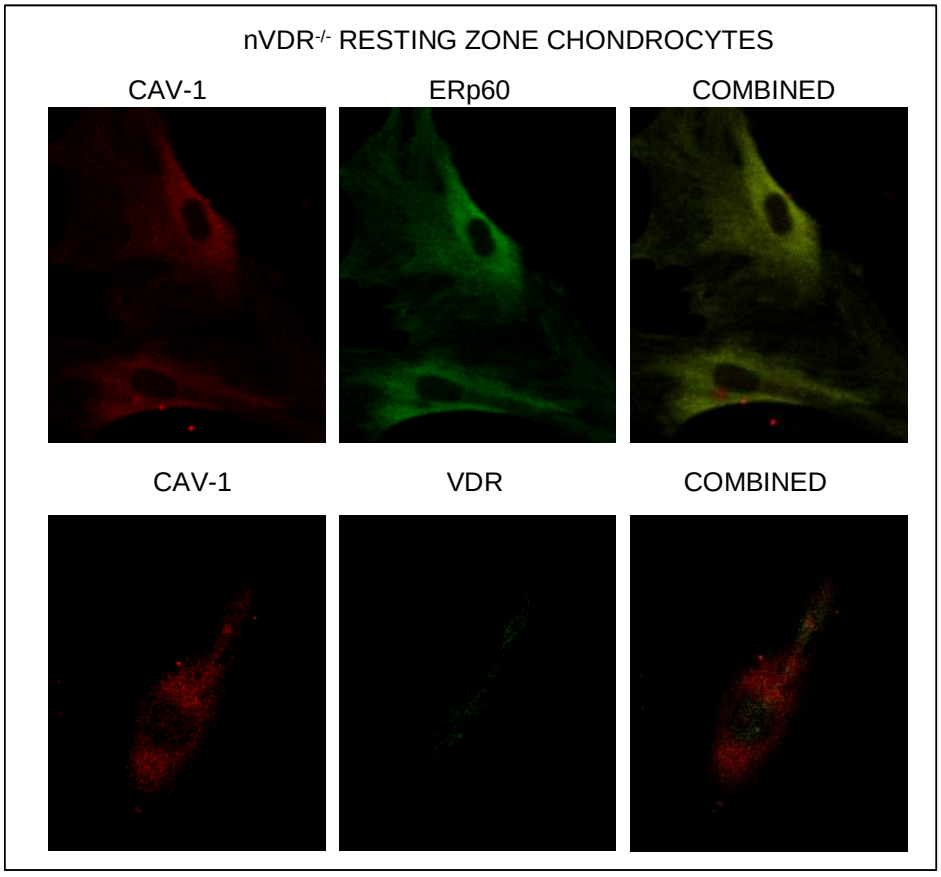

Figure 21. Laser scanning confocal microscopy of rat RC VDR$^{-/-}$ chondrocytes demonstrating subcellular localization of caveolin-1 and ERp60 or caveolin-1 and VDR. Result was found in over 50% of the cells examined.

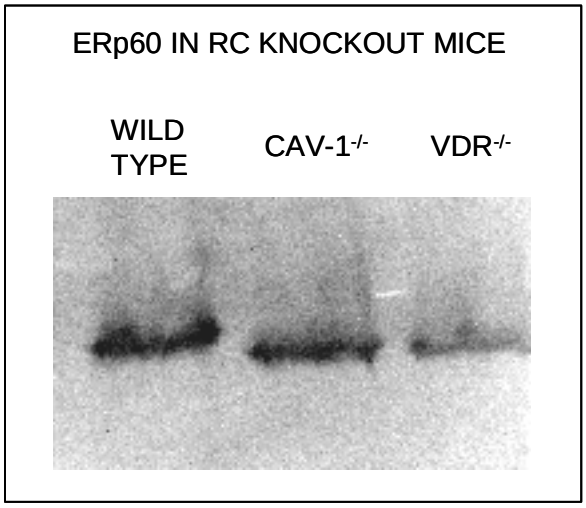

Figure 22. Western Blot showing the presence of ERp60 in RC wild type chondrocytes, Cav-$1^{-/-}$ chondrocytes, and $VDR^{-/-}$ chondrocytes.

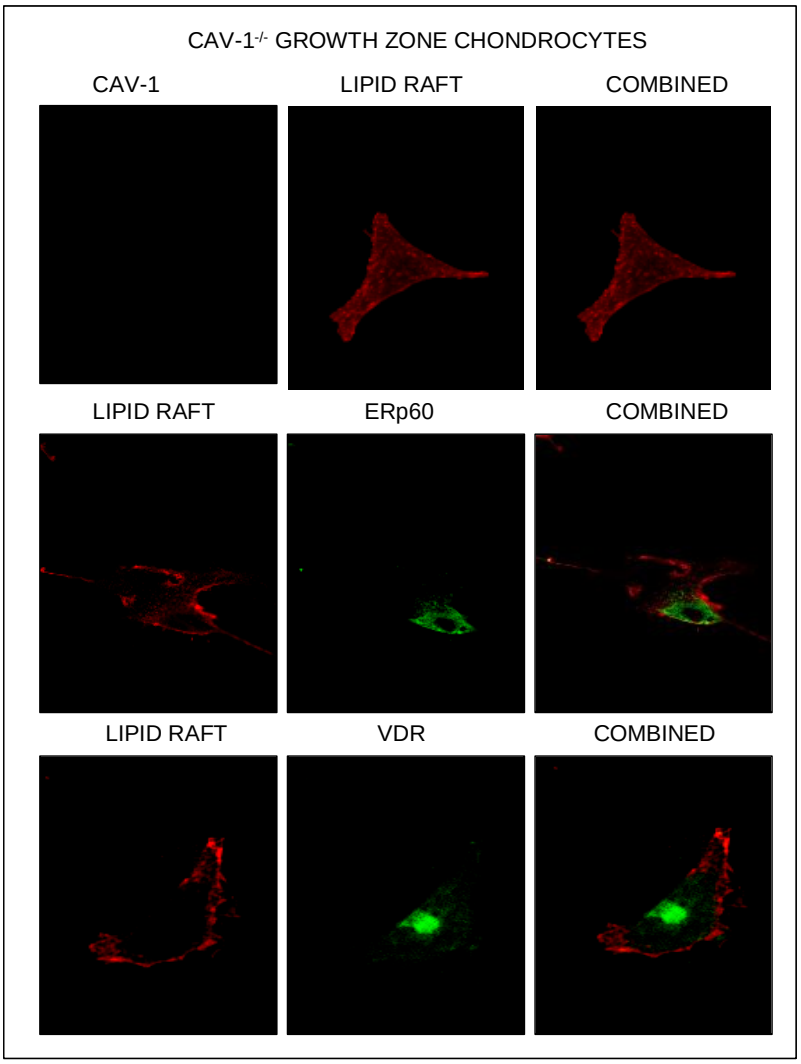

Figure 23. Laser scanning confocal microscopy of rat GC Cav-1$^{-/-}$ chondrocytes demonstrating subcellular localization of lipid rafts and cavelon-1, lipid rafts and ERp60, or lipid rafts and the nuclear VDR. Result was found in over 50% of the cells examined.

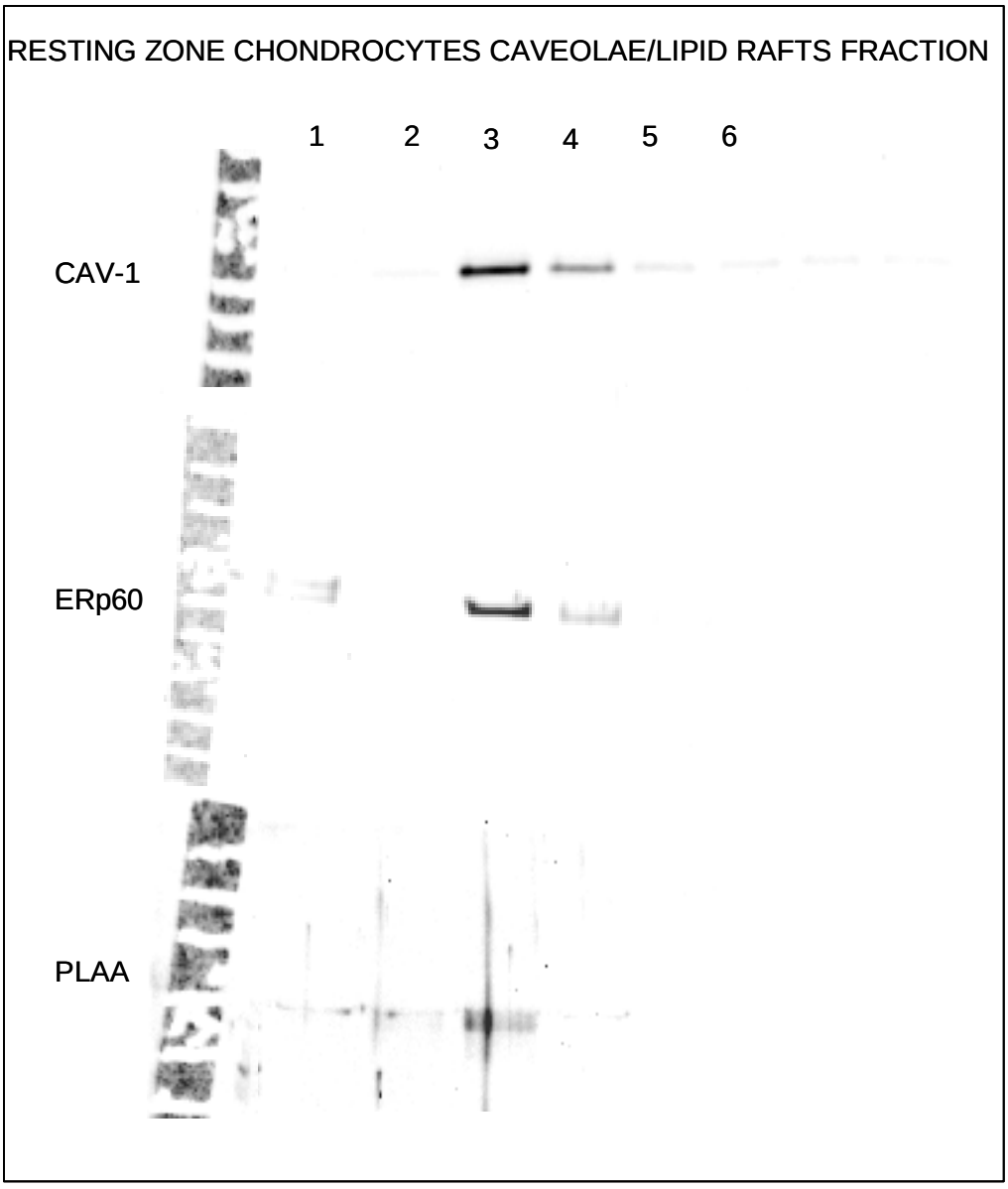

Figure 24. Western Blot of caveolin-1-rich caveolae/lipid raft fractions from RC cells. Fraction 3 denotes caveolae/lipid raft fraction. ERp60 and PLAA were found to co-fractionate with caveolin-1 in RC cells.

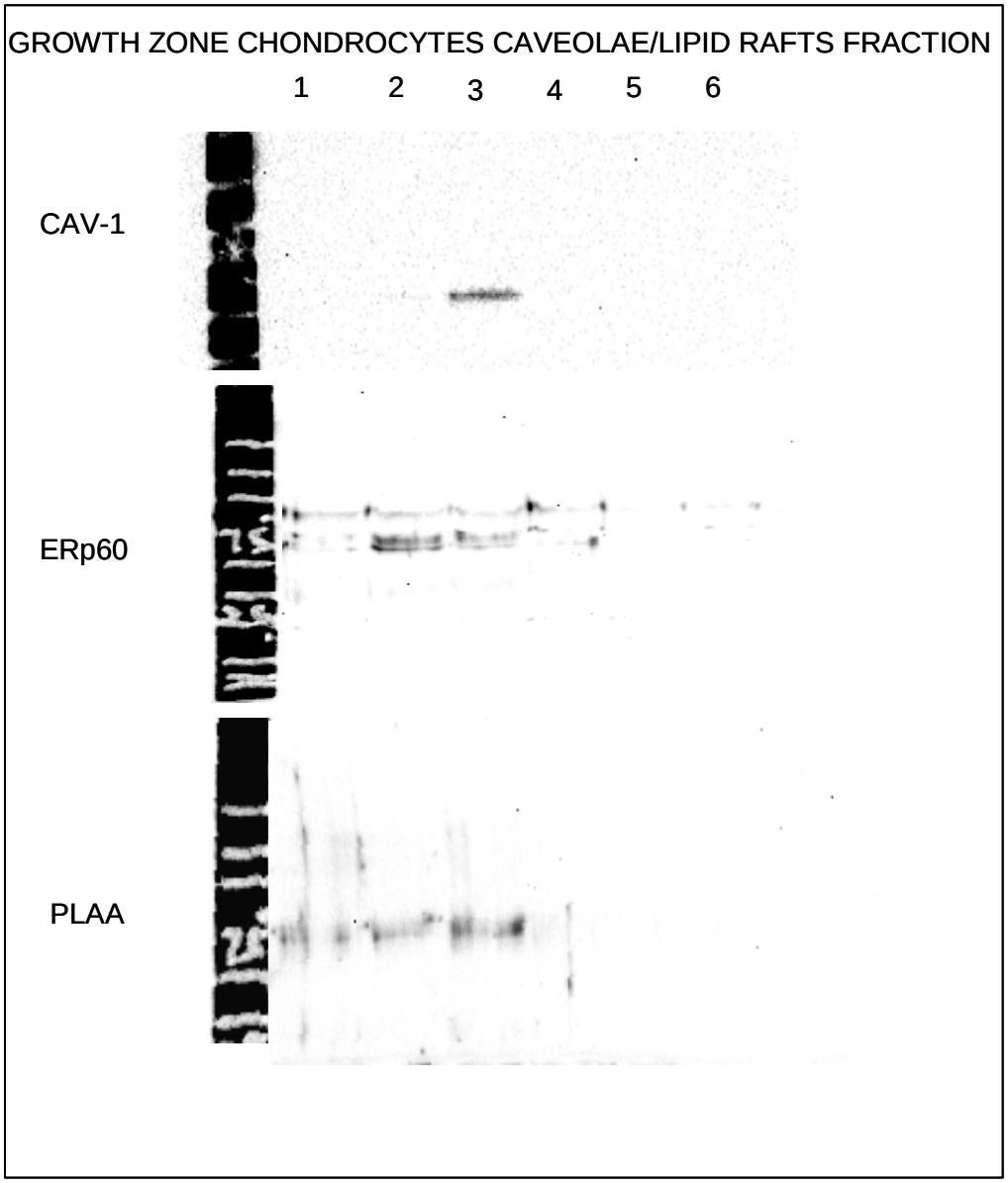

Figure 25. Western Blot of caveolin-1-rich caveolae/lipid raft fractions from rat GC cells. Fraction 3 denotes caveolae/lipid raft fraction. ERp60 and PLAA were found to co-fractionate with caveolin-1 in GC cells.

CHAPTER 4. DISCUSSION

Caveolin-1$^{-/-}$ mice have systemic changes due to alterations in several caveolae-dependent cellular mechanisms. These include the previously shown pulmonary and vascular alterations [47]. The experiments performed here show that there is also significant dependence of the skeletal system on caveolae and Cav-1. Our study shows that skeletal phenotype and development are significantly dependent on the presence of Cav-1. In addition to the increase in bone volume and MAR in Cav-1$^{-/-}$ mice, additional studies (not shown here) show that Cav-1 deletion also leads to stiffer bone. Studies in collaboration with Rubin et al. have shown that the pronounced Cav-1$^{-/-}$ phenotype was found in the metaphysis and not in the epiphysis. This may possibly be due to the development of the epiphysis in the earlier stages of development whereas the metaphysis undergoes dynamic re-modeling in post-fetal mice.

Histomorphometric studies of the growth plate also show that there are significant differences in Cav-1$^{-/-}$ animals. While there are similarities between Cav-1$^{-/-}$ and VDR$^{-/-}$ mice, such as the expansion of the hypertrophic cartilage [49], the greater increase in cell number in the columns is due to a failure in closure as opposed to the failure in mineralization seen in rickets. Even though Cav-1$^{-/-}$ mice do not exhibit the same growth plate phenotype as VDR$^{-/-}$ mice, many components integral to vitamin D effects in PKC signaling have been found to localize within caveolae.

The studies show that Cav-1 has a definite and important role in skeletal development and formation. However, it is still not clear if the phenotype observed in Cav-1$^{-/-}$ mice is due to a direct change in cellular mechanisms that regulate the phenotype or if it is indirectly due to other systematic changes caused through intermediate

mechanisms. To clarify the role of caveolae on a cellular level, we focused on the vitamin D pathway through caveolae and lipid rafts in chondrocytes. This is due to the localization of important components in vitamin D signaling such as PLA_2, DAG, PKC, and VDR in caveolae [38, 41-45]. Additionally, vitamin D has been shown to be a very important regulator of the growth plate [59], thus indicating a correlation between the phenotype observed in Cav-$1^{-/-}$ mouse with an altered vitamin D signaling cascade.

RC and GC cells are different in differentiation, cellular phenotype, and response to 1α,25$(OH)_2D_3$ and 24,25$(OH)_2D_3$. It is then expected that they would have different properties in relation to vitamin D signaling and caveolae. While the protein expression of caveolins 1, 2, and 3 did not differ significantly, the amount and size of the caveolae in GC and RC cells varied. These differences may correlate with differences observed between the membrane fluidity of the cells [23], since caveolae and their increased levels of cholesterol and the difference in lipid composition are involved in the "liquid-ordered" characteristic of the caveolae membrane domains as opposed to the traditional "liquid-disordered" characteristics of the phospholipid membranes. RC and GC cells also respond differently to 1α,25$(OH)_2D_3$ and 24,25$(OH)_2D_3$, thus contributing to a different dependence of caveolae-associated mechanisms. Caveolae levels have also been associated with cellular differentiation, which might explain why Cav-$1^{-/-}$ mice have more hypertrophic cells but not more proliferative cells. However, the association of caveolae with differentiation is varied as some cells show increases in proliferation while others do not [60-62].

While ERp60 is implicated as a membrane receptor for 1α,25$(OH)_2D_3$ in GC cells, its role in RC cells is not yet elucidated. Previous work has shown that the

membrane action of 1α,25$(OH)_2D_3$ and 24,25$(OH)_2D_3$ are retained in growth plate cartilage cells from $VDR^{-/-}$ mice [5]. This indicates that a distinctive receptor is responsible for 24,25$(OH)_2D_3$ membrane effects just as ERp60 is responsible for 1α,25$(OH)_2D_3$ membrane action. A specific receptor for 24,25$(OH)_2D_3$ isolated from chick lysosomal membranes has been proposed as the membrane receptor responsible for stimulating PKC activity via a mechanism that involves PLD but not PLC or PLA_2 [63]. However, it is not certain that 1α,25$(OH)_2D_3$ and 24,25$(OH)_2D_3$ function via different receptors. 1α,25$(OH)_2D_3$ and 24,25$(OH)_2D_3$ have physiochemical properties [22, 64] that may allow different vitamin D metabolites to interact very differently to the same receptor, ERp60. To identify the potential role of ERp60 in RC cells, we also examined the location and the interaction of different components of vitamin D membrane action in RC cells.

Using β-CD, our study confirms the important role of intact caveolae for rapid activation of PKC via vitamin D. β-CD alters the physical structure of lipid rafts and caveolae by displacing cholesterol, and it also inhibits the stimulatory effects of 1α,25$(OH)_2D_3$. The number of caveolae were reduced significantly when cells were treated with β-CD, but some caveolae were still present, as has been noted previously for endothelial cells after treatment with β-CD [52]. Western blot analysis show that in both RC and GC cells treated with β-CD, the amount of ERp60, VDR, and Cav-1 did not decrease significantly. This supports the mechanism of β-CD, and indicates that the amount of functional protein was not reduced by β-CD, supporting the conclusion that caveolae are important domains responsible for the membrane action of vitamin D. In the cholesterol depleted environment, it is possible that β-CD replaces the cholesterol-

derived vitamin D metabolite. Additionally, our study shows that by itself, β-CD did not affect PKC in control cultures, indicating that its action was specific to the requirements for $1\alpha,25(OH)_2D_3$-dependent activation of the enzyme. Studies have shown that cytosolic PLA_2 and PLC-β are both upstream of the PKC response to $1\alpha,25(OH)_2D_3$, and they have been found to localize in caveolae of other systems [41, 42]. This suggests that the scaffolding of these enzymes is important for the observed $1\alpha,25(OH)_2D_3$ effect. Our data also show that the lack of a membrane-mediated response also has downstream consequences. Pre-treatment of GC cells with β-CD reduced the stimulatory effects of $1\alpha,25(OH)_2D_3$ on alkaline phosphatase activity and [^{35}S]sulfate incorporation. It is unlikely that this result is due to the toxic effects of β-CD. Cells were treated with β-CD for 30 min and then followed by fresh media with $1\alpha,25(OH)_2D_3$. These results confirm the substantive role of caveolae as a vital structure in both the rapid action of vitamin D as seen in PKC activation but also downstream effects as seen in alkaline phosphatase activity and [^{35}S]sulfate incorporation.

Using Cav-$1^{-/-}$ cells, we were able to confirm the conclusion from β-CD treatments. Caveolin-1 is a major scaffolding protein for caveolae [65, 66], and growth plate cartilage cells from Cav-$1^{-/-}$ mice were found to lack detectable protein via Western blot and there were no visible caveolae structures. We checked to confirm the expression of ERp60 in Cav-$1^{-/-}$ cells. Even though ERp60 is present in the absence of caveolin-1 or intact caveolae, the characteristic effects of $1\alpha,25(OH)_2D_3$ via ERp60 were not seen. The rapid membrane action as observed through PKC activity was reduced, similar to pre-treatment of cells with β-CD. The observed downstream action of $1\alpha,25(OH)_2D_3$ as seen

through alkaline phosphatase activity and [^{35}S]sulfate incorporation was also significantly reduced.

It is possible that the classical VDR is involved in rapid PKC activation. While VDR knockout mice contain truncated versions of VDR [67], which contains the 1α,25$(OH)_2D_3$ binding site but lacks the DNA recognition site. Cells isolated from VDR$^{-/-}$ mice continue to exhibit rapid response to 1α,25$(OH)_2D_3$ and 24,25$(OH)_2D_3$, despite having a non-functional VDR [5]. While we cannot rule out a contradiction from the truncated receptor, it is clear that VDR-dependant mRNA is not required for many of the 1α,25$(OH)_2D_3$ and 24,25$(OH)_2D_3$ effects in these cells. Confocal effects microscopy shows VDR and ERp60 have distinctive cellular compartmentalization. While VDR was found in the nucleus and the perinuclear regions, ERp60 was noticeably absent from the nucleus, which may be indicative of its nongenomic role. Caveolin-1 and lipid raft staining show a similar localization in the membrane and the perinuclear regions including the Golgi and the endoplasmic reticulum. It is possible that endoplasmic reticulum, the site for membrane biogenesis, is the initiating site for the eventual co-localization of ERp60 with Cav-1 and lipid rafts. The co-localization between ERp60 and Cav-1 was also found via Western blots. The distinction between ERp60 and VDR is evident through plasma membrane and matrix vesicle fractions. While ERp60 is found in whole cell lysates, plasma membrane, and matrix vesicles, VDR is noticeably absent from plasma membrane and matrix vesicles. ERp60 is located in similar locations and fractions in RC and GC cells. This provides potential evidence that ERp60 is able to bind to both 1α,25$(OH)_2D_3$ and 24,25$(OH)_2D_3$, albeit via different pathways that lead to PKC

activation. We are able to conclusively determine that in our system, rat cartilage cells, ERp60 is a component of caveolae while VDR is not.

Others have shown that VDR is located in caveolae enriched membrane preparations in other cell types [38]. It is possible that VDR is able to shuttle in and out of caveolae. It has been shown that VDR is located adjacent to plasma membranes in $1\alpha,25(OH)_2D_3$-trated cells [69], suggesting that under certain physiological conditions, VDR may become associated with lipid rafts or caveolae. Confocal microscopy of $VDR^{-/-}$ GC cells shows the co-localization between ERp60 and lipid rafts remains in the absence of functional VDR. Additionally, Cav-$1^{-/-}$ GC cells show the specific localization of ERp60 is in caveolae since the localization in lipid rafts is absent without intact caveolae.

$1\alpha,25(OH)_2D_3$ and $24,25(OH)_2D_3$ regulate PKC activity in matrix vesicles during matrix vesicle biogenesis through cellular mechanisms. Additionally, $1\alpha,25(OH)_2D_3$ and $24,25(OH)_2D_3$ can also regulate matrix vesicles through direct actions [70]. When GC cells are treated with $1\alpha,25(OH)_2D_3$ or RC cells are treated with $24,25(OH)_2D_3$, PKC activity in the extracellular organelle is increased through specific incorporation of PKCζ. PKCζ is an atypical form of PKC that does not require either lipid or Ca^{2+} as cofactors. While PKC increases due to PKCζ, the direct effect of $1\alpha,25(OH)_2D_3$ and $24,25(OH)_2D_3$ on matrix vesicles by the target cells inhibit PKCζ specifically [70]. This finding suggests that vitamin D metabolites influence cells and matrix vesicles through very different mechanisms. Western blot analysis shows that both ERp60 and Cav-1 are present in matrix vesicles while VDR is absent. While the role of ERp60 and Cav-1 in matrix vesicles is not clear, it has been found that $1\alpha,25(OH)_2D_3$ can directly increase

PLA_2 activity in matrix vesicles [30]. The resulting release of lysophospholipids also participates in the release and activation of latent TGF-β1 [71]. This is likely due to a change in the detergent properties either through a loss of membrane integrity leading to release of MMP-3 or by the disruption of the three dimensional structure of the extracellular matrix [70].

PLA_2 has a prominent role in vitamin D signaling. PLA_2 is involved in $1\alpha,25(OH)_2D_3$ and $24,25(OH)_2D_3$ signaling even though the metabolites activate PKC in different pathways. Additionally, while matrix vesicles and plasma membranes have different vitamin D signaling mechanisms, the involvement of PLA_2 is vital. Studies have shown localization of PLA_2 in caveolae [41]. Further clues into the role of caveolae in vitamin D signaling may lie in PLAA, an activator of PLA_2. Caveolae fraction shows that PLAA localizes in caveolin-1- and ERp60-rich fractions. In collaboration with studies that show PLAA may be a G protein and studies that show localization of PLA_2 in caveolae, caveolae may be the location where vitamin D membrane signaling is initiated through activation of PLAA.

CHAPTER 5. CONCLUSIONS AND FUTURE DIRECTIONS

Researchers have increasingly studied the potential of vitamin D metabolites in many disease states in the human body. While vitamin D and its metabolites have shown an ability to regulate different disease states, changes in vitamin D levels have a direct effect on calcium balance in the system. Analogues that act differently via VDR have been studied extensively. However, very little is known about the membrane receptor for $1\alpha,25(OH)_2D_3$, ERp60. In our study, we seek to provide clarification of how ERp60 is able to rapidly increase PKC activity. We were able to distinguish localization and function for ERp60 and VDR. Caveolae and Cav-1 are vital for the normal localization and function of ERp60. The differences between ERp60 and VDR provide a clue into future targets in the treatment of diseases. Lastly, a potential target, PLAA in the caveolae domains, has been identified as an early component of the membrane-based vitamin D signaling.

Further clarification of the differences between ERp60 and VDR is needed. While ERp60 and VDR are distinct proteins, ERp60 is also a scaffolding protein involved in the formation of disulfide bonds. It is possible ERp60 functions in collaboration with VDR to exert $1\alpha,25(OH)_2D_3$-dependent membrane effects. Also, the contradiction between the location of VDR and caveolae in our studies and other studies may be indicative of the ability for VDR to shuttle in and out of membrane domains. To further clarify the role of ERp60, future studies will include studying the effects of conditionally knocking out the ERp60 gene in animals.

Caveolae and Cav-1 are vital for ERp60 localization and function, and the membrane effects of $1\alpha,25(OH)_2D_3$ initiate in the caveolae domains through the

localization of PLAA. While the localization of components in ERp60 functional pathway is clear, the interactions of these components are not yet clear. While PLAA is localized in the caveolae domains, it is not clear if PLAA directly interacts with Cav-1, ERp60, or indirectly through another molecule. Lastly, it is possible that activation of PLAA results in the release of PLAA to activate PLA_2 in other areas in the membrane. Immunoprecipitation in conjunction with varying levels of serum vitamin D and its metabolites can indicate the interaction of ERp60 with caveolae.

In summary, we believe that caveolae are vital domains for membrane effects of vitamin D. Without the caveolae domains, ERp60 is unable to elicit the same biological response seen in cells with functional caveolae. It is unclear the mechanism with which ERp60 interacts with caveolae and caveolin-1, but the interaction between them leads to the biological responses observed. We further observe that the localization of PLA_2 may provide a direct link between the interactions between ERp60 and vitamin D in caveolae to the down stream effects we observed.

We have established a cellular target for studying and examining the role of ERp60. Future efforts will focus on these membrane domains and the initiation of signaling through PLAA. With the significant role of vitamin D metabolites in bone development, cancer, cardiovascular diseases, and immune system, the potential in using ERp60 and its signaling pathway as a therapeutic target is tremendous.

REFERENCES

1. Cantorna, M.T., *Vitamin D and its role in immunology: multiple sclerosis, and inflammatory bowel disease.* Prog Biophys Mol Biol, 2006. **92**(1): p. 60-4.

2. Schwartz, G.G. and H.G. Skinner, *Vitamin D status and cancer: new insights.* Curr Opin Clin Nutr Metab Care, 2007. **10**(1): p. 6-11.

3. Boyan, B.D., et al., *1,25-(OH)2D3 modulates growth plate chondrocytes via membrane receptor-mediated protein kinase C by a mechanism that involves changes in phospholipid metabolism and the action of arachidonic acid and PGE2.* Steroids, 1999. **64**(1-2): p. 129-36.

4. Barbara D Boyan, Z.S., David S Howell, Michael Naski, Don M Ranly, Victor L Silvia, David D Dean, *Biology, Chemistry, and Biochemistry of the Mammalian Growth Plate*, in *Disorders of Bone and Mineral Metabolism*, M.J.F. Fredric L Coe, Editor. 2002, Lippincott Williams & Wilkins: Philadelphia. p. 255-314.

5. Boyan, B.D., et al., *Membrane actions of vitamin D metabolites 1alpha,25(OH)2D3 and 24R,25(OH)2D3 are retained in growth plate cartilage cells from vitamin D receptor knockout mice.* J Cell Biochem, 2003. **90**(6): p. 1207-23.

6. Boyan, B.D., et al., *The effects of vitamin D metabolites on the plasma and matrix vesicle membranes of growth and resting cartilage cells in vitro.* Endocrinology, 1988. **122**(6): p. 2851-60.

7. Nemere, I., et al., *Identification and characterization of 1,25D3-membrane-associated rapid response, steroid (1,25D3-MARRS) binding protein.* J Steroid Biochem Mol Biol, 2004. **89-90**(1-5): p. 281-5.

8. St-Arnaud, R., G.A. Candeliere, and S. Dedhar, *New mechanisms of regulation of the genomic actions of vitamin D in bone cells: interaction of the vitamin D receptor with non-classical response elements and with the multifunctional protein, calreticulin.* Front Biosci, 1996. **1**: p. d177-88.

9. Barbara D Boyan, Z.S., Wallace H Coulter, *Cartilage and Vitamin D: Genomic and Nongenomic Regulation by 1,25(OH)$_2$D$_3$ and 24,25(OH)$_2$D$_3$*, in *Vitamin D*, F.H.G. David Feldman, J Wesley Pike, Editor. 1997, Academic Press: London. p. 577-598.

10. Buckwalter, J.A., et al., *Morphometric analysis of chondrocyte hypertrophy.* J Bone Joint Surg Am, 1986. **68**(2): p. 243-55.

11. Howell, D.S. and L. Carlson, *Alterations in the composition of growth cartilage septa during calcification studied by microscopic x-ray elemental analysis.* Exp Cell Res, 1968. **51**(1): p. 185-95.

12. Seo, E.G., T.A. Einhorn, and A.W. Norman, *24R,25-dihydroxyvitamin D3: an essential vitamin D3 metabolite for both normal bone integrity and healing of tibial fracture in chicks.* Endocrinology, 1997. **138**(9): p. 3864-72.

13. Plachot, J.J., et al., *In vitro action of 1,25-dihydroxycholecalciferol and 24,25-dihydroxycholecalciferol on matrix organization and mineral distribution in rabbit growth plate.* Metab Bone Dis Relat Res, 1982. **4**(2): p. 135-42.

14. Parfitt, A.M., et al., *Calcitriol but no other metabolite of vitamin D is essential for normal bone growth and development in the rat.* J Clin Invest, 1984. **73**(2): p. 576-86.

15. Sylvia, V.L., et al., *Maturation-dependent regulation of protein kinase C activity by vitamin D3 metabolites in chondrocyte cultures.* J Cell Physiol, 1993. **157**(2): p. 271-8.

16. Sylvia, V.L., et al., *Nongenomic regulation of protein kinase C isoforms by the vitamin D metabolites 1 alpha,25-(OH)2D3 and 24R,25-(OH)2D3.* J Cell Physiol, 1996. **167**(3): p. 380-93.

17. Nemere, I., et al., *Identification of a membrane receptor for 1,25-dihydroxyvitamin D3 which mediates rapid activation of protein kinase C.* J Bone Miner Res, 1998. **13**(9): p. 1353-9.

18. Pedrozo, H.A., et al., *Physiological importance of the 1,25(OH)2D3 membrane receptor and evidence for a membrane receptor specific for 24,25(OH)2D3.* J Bone Miner Res, 1999. **14**(6): p. 856-67.

19. Muller, S.A., A.S. Posner, and H.E. Firschein, *Effect of vitamin D deficiency on the crystal chemistry of bone mineral.* Proc Soc Exp Biol Med, 1966. **121**(3): p. 844-6.

20. Li, Y.C., et al., *Normalization of mineral ion homeostasis by dietary means prevents hyperparathyroidism, rickets, and osteomalacia, but not alopecia in vitamin D receptor-ablated mice.* Endocrinology, 1998. **139**(10): p. 4391-6.

21. Roughley, P.J. and I.R. Dickson, *A comparison of proteoglycan from chick cartilage of different types and a study of the effect of vitamin D on proteoglycan structure.* Connect Tissue Res, 1986. **14**(3): p. 187-97.

22. Kato, A., et al., *Studies on 24R,25-dihydroxyvitamin D3: evidence for a nonnuclear membrane receptor in the chick tibial fracture-healing callus.* Bone, 1998. **23**(2): p. 141-6.

23. Putkey, J.A., et al., *Vitamin D-mediated intestinal calcium transport. Effects of essential fatty acid deficiency and spin label studies of enterocyte membrane lipid fluidity.* Biochim. Biophys. Acta. 1982. **688**(1): p. 177-90.

24. Swain, L.D., et al., *Nongenomic regulation of chondrocyte membrane fluidity by 1,25-(OH)2D3 and 24,25-(OH)2D3 is dependent on cell maturation.* Bone, 1993. **14**(4): p. 609-17.

25. Helm, S., et al., *24,25-(OH)2D3 regulates protein kinase C through two distinct phospholipid-dependent mechanisms.* J Cell Physiol, 1996. **169**(3): p. 509-21.

26. Schwartz, Z., et al., *1alpha,25-dihydroxyvitamin D(3) and 24R,25-dihydroxyvitamin D(3) modulate growth plate chondrocyte physiology via protein kinase C-dependent phosphorylation of extracellular signal-regulated kinase 1/2 mitogen-activated protein kinase.* Endocrinology, 2002. **143**(7): p. 2775-86.

27. Schwartz, Z., et al., *The effect of 24R,25-(OH)(2)D(3) on protein kinase C activity in chondrocytes is mediated by phospholipase D whereas the effect of 1alpha,25-(OH)(2)D(3) is mediated by phospholipase C.* Steroids, 2001. **66**(9): p. 683-94.

28. Schwartz, Z., et al., *1alpha,25(OH)2D3 causes a rapid increase in phosphatidylinositol-specific PLC-beta activity via phospholipase A2-dependent production of lysophospholipid.* Steroids, 2003. **68**(5): p. 423-37.

29. Boyan, B.D., et al., *1alpha,25(OH)2D3 is an autocrine regulator of extracellular matrix turnover and growth factor release via ERp60 activated matrix vesicle metalloproteinases*
Journal of Steroid Biochemistry & Molecular Biology, 2006. **Article in press**.

30. Schwartz, Z., et al., *Direct effects of 1,25-dihydroxyvitamin D3 and 24,25-dihydroxyvitamin D3 on growth zone and resting zone chondrocyte membrane alkaline phosphatase and phospholipase-A2 specific activities.* Endocrinology, 1988. **123**(6): p. 2878-84.

31. Simons, K. and D. Toomre, *Lipid rafts and signal transduction.* Nat Rev Mol Cell Biol, 2000. **1**(1): p. 31-9.

32. Lisanti, M.P., et al., *Characterization of caveolin-rich membrane domains isolated from an endothelial-rich source: implications for human disease.* J Cell Biol, 1994. **126**(1): p. 111-26.

33. Smart, E.J., et al., *A detergent-free method for purifying caveolae membrane from tissue culture cells.* Proc Natl Acad Sci U S A, 1995. **92**(22): p. 10104-8.

34. Schwab, W., et al., *Characterization of caveolins from human knee joint catilage: expression of caveolin-1, -2, and -3 in chondrocytes and association with integrin beta1.* Histochem Cell Biol, 2000. **113**(3): p. 221-5.

35. Cameron, P.L., et al., *Identification of caveolin and caveolin-related proteins in the brain.* J Neurosci, 1997. **17**(24): p. 9520-35.

36. Parton, R.G., *Cell biology. Life without caveolae.* Science, 2001. **293**(5539): p. 2404-5.

37. Razani, B., S.E. Woodman, and M.P. Lisanti, *Caveolae: from cell biology to animal physiology.* Pharmacol Rev, 2002. **54**(3): p. 431-67.

38. Huhtakangas, J.A., et al., *The vitamin D receptor is present in caveolae-enriched plasma membranes and binds 1 alpha,25(OH)2-vitamin D3 in vivo and in vitro.* Mol Endocrinol, 2004. **18**(11): p. 2660-71.

39. Deecher, D.C., et al., *Characterization of a membrane-associated estrogen receptor in a rat hypothalamic cell line (D12).* Endocrine, 2003. **22**(3): p. 211-23.

40. Zhang, X., et al., *Caveolin-1 down-regulation activates estrogen receptor alpha expression and leads to 17beta-estradiol-stimulated mammary tumorigenesis.* Anticancer Res, 2005. **25**(1A): p. 369-75.

41. Graziani, A., et al., *Cholesterol- and caveolin-rich membrane domains are essential for phospholipase A2-dependent EDHF formation.* Cardiovasc Res, 2004. **64**(2): p. 234-42.

42. Yamaga, M., et al., *A PLCdelta1-binding protein, p122/RhoGAP, is localized in caveolin-enriched membrane domains and regulates caveolin internalization.* Genes Cells, 2004. **9**(1): p. 25-37.

43. Garver, W.S., et al., *The Npc1 mutation causes an altered expression of caveolin-1, annexin II and protein kinases and phosphorylation of caveolin-1 and annexin II in murine livers.* Biochim Biophys Acta, 1999. **1453**(2): p. 193-206.

44. Goudenege, S., et al., *Biologically active milli-calpain associated with caveolae is involved in a spatially compartmentalised signalling involving protein kinase C alpha and myristoylated alanine-rich C-kinase substrate (MARCKS).* Int J Biochem Cell Biol, 2005. **37**(9): p. 1900-10.

45. Peitsch, M.C., C. Borner, and J. Tschopp, *Sequence similarity of phospholipase A2 activating protein and the G protein beta-subunits: a new concept of effector protein activation in signal transduction?* Trends Biochem Sci, 1993. **18**(8): p. 292-3.

46. Razani, B., et al., *Caveolin-1-deficient mice are lean, resistant to diet-induced obesity, and show hypertriglyceridemia with adipocyte abnormalities.* J Biol Chem, 2002. **277**(10): p. 8635-47.

47. Drab, M., et al., *Loss of caveolae, vascular dysfunction, and pulmonary defects in caveolin-1 gene-disrupted mice.* Science, 2001. **293**(5539): p. 2449-52.

48. Chen, C.H., Y. Sakai, and M.B. Demay, *Targeting expression of the human vitamin D receptor to the keratinocytes of vitamin D receptor null mice prevents alopecia.* Endocrinology, 2001. **142**(12): p. 5386-9.

49. Li, Y.C., et al., *Targeted ablation of the vitamin D receptor: an animal model of vitamin D-dependent rickets type II with alopecia.* Proc Natl Acad Sci U S A, 1997. **94**(18): p. 9831-5.

50. Donohue, M.M. and M.B. Demay, *Rickets in VDR null mice is secondary to decreased apoptosis of hypertrophic chondrocytes.* Endocrinology, 2002. **143**(9): p. 3691-4.

51. Parfitt, A.M., et al., *Bone histomorphometry: standardization of nomenclature, symbols, and units. Report of the ASBMR Histomorphometry Nomenclature Committee.* J Bone Miner Res, 1987. **2**(6): p. 595-610.

52. Park, H., et al., *Plasma membrane cholesterol is a key molecule in shear stress-dependent activation of extracellular signal-regulated kinase.* J Biol Chem, 1998. **273**(48): p. 32304-11.

53. Schnitzer, J.E., et al., *Filipin-sensitive caveolae-mediated transport in endothelium: reduced transcytosis, scavenger endocytosis, and capillary permeability of select macromolecules.* J Cell Biol, 1994. **127**(5): p. 1217-32.

54. Schwartz, Z., et al., *Effects of vitamin D metabolites on collagen production and cell proliferation of growth zone and resting zone cartilage cells in vitro.* J Bone Miner Res, 1989. **4**(2): p. 199-207.

55. Bell, R.M., Y. Hannun, and C. Loomis, *Mixed micelle assay of protein kinase C.* Methods Enzymol, 1986. **124**: p. 353-9.

56. Conrad, P.A., et al., *Caveolin cycles between plasma membrane caveolae and the Golgi complex by microtubule-dependent and microtubule-independent steps.* J Cell Biol, 1995. **131**(6 Pt 1): p. 1421-33.

57. Scherer, P.E., et al., *Identification, sequence, and expression of caveolin-2 defines a caveolin gene family.* Proc Natl Acad Sci U S A, 1996. **93**(1): p. 131-5.

58. Song, K.S., et al., *Expression of caveolin-3 in skeletal, cardiac, and smooth muscle cells. Caveolin-3 is a component of the sarcolemma and co-fractionates with dystrophin and dystrophin-associated glycoproteins.* J Biol Chem, 1996. **271**(25): p. 15160-5.

59. Boyan, B.D., et al., *Mechanisms regulating differential activation of membrane-mediated signaling by 1alpha,25(OH)2D3 and 24R,25(OH)2D3.* J Steroid Biochem Mol Biol, 2004. **89-90**(1-5): p. 309-15.

60. Galbiati, F., et al., *Caveolin-1 expression inhibits Wnt/beta-catenin/Lef-1 signaling by recruiting beta-catenin to caveolae membrane domains.* J Biol Chem, 2000. **275**(30): p. 23368-77.

61. Razani, B., et al., *Caveolin-1 null mice are viable but show evidence of hyperproliferative and vascular abnormalities.* J Biol Chem, 2001. **276**(41): p. 38121-38.

62. Williams, T.M. and M.P. Lisanti, *Caveolin-1 in oncogenic transformation, cancer, and metastasis.* Am J Physiol Cell Physiol, 2005. **288**(3): p. C494-506.

63. Nemere, I., et al., *Characterization of 1,25D3-membrane assocated rapid response, steroid binding (1,25D3-MARRS) protein from the domestic chicken.* Mole Biol Cell, 2003. **12** (Supplement).

64. Seo, E.G., T.A. Einhorn, and A.W. Norman, *24R-25dihydroxyvitamin D3: An essential vitamin D3 metabolite for both normal bone integrity and healing of tibial fracture in chicks.* J Bone Miner Res, 1996. **11**(S): p. 422.

65. van Deurs, B., et al., *Caveolae: Anchored, multifunctional platforms in the lipid ocean.* Trends Cell Biol, 2003. **13**: p. 92-100.

66. Shaw, P.W. and R.G. Anderson, *Role of plasmalemnal caveolae in signal transduction.* Am J Physiol, 1998. **275**: p. L843-L851.

67. Bula, C.M., et al., *Presence of a truncated form of the vitamin D receptor (VDR) in a strain of VDR-knockout mice.* Endocrinology, 2005. **146**(12): p. 5581-6.

68. Wali, R.K., et al., *Vitamin D receptor is not required for the rapid actions of 1,25-dihydroxyvitamin D3 to increase intracellular calcium and activate protein kinase C in mouse osteoblasts.* J Cell Biochem, 2003. **88**(4): p. 794-801.

69. Kim, Y.S., et al., *Association of 1 alpha,25-dihydroxyvitamin D3-occupied vitamin D receptors with cellular membrane acceptance sites.* Endocrinology, 1996. **137**(9): p. 3649-58.

70. Boyan, B.D., et al., *1alpha,25(OH)(2)D(3) is an autocrine regulator of extracellular matrix turnover and growth factor release via ERp60 activated matrix vesicle metalloproteinases.* J Steroid Biochem Mol Biol, 2007.

71. Gay, I., et al., *Lysophospholipid regulates release and activation of latent TGF-beta1 from chondrocyte extracellular matrix.* Biochim Biophys Acta, 2004. **1684**(1-3): p. 18-28.